AUTOMATED PROTOCOL FOR ANALYSIS OF DYNAMIC MECHANICAL ANALYZER DATA FROM FINE AGGREGATE ASPHALT MIXES

A Thesis

by

PEDRO CAVALCANTI DE SOUSA

Submitted to the Office of Graduate Studies of
Texas A&M University
in partial fulfillment of the requirements for the degree of

MASTER OF SCIENCE

August 2010

Major Subject: Civil Engineering

AUTOMATED PROTOCOL FOR ANALYSIS OF DYNAMIC MECHANICAL ANALYZER DATA FROM FINE AGGREGATE ASPHALT MIXES

A Thesis

by

PEDRO CAVALCANTI DE SOUSA

Submitted to the Office of Graduate Studies of
Texas A&M University
in partial fulfillment of the requirements for the degree of

MASTER OF SCIENCE

Approved by:

Co-Chairs of Committee,	Dallas N. Little
	Eyad Masad
Committee Member,	Charles J. Glover
Head of Department,	John Niedzwecki

August 2010

Major Subject: Civil Engineering

ABSTRACT

Automated Protocol for Analysis of Dynamic Mechanical
Analyzer Data from Fine Aggregate Asphalt Mixes. (August 2010)
Pedro Cavalcanti De Sousa, B.E., Federal University of Ceara, Brazil; M.E., Ecole
Centrale de Lyon, France.
Co-Chairs of Advisory Committee, Dr. Dallas N. Little
Dr. Eyad Masad

Fatigue cracking and moisture damage are two important modes of distress in asphalt pavements. Recently, the Dynamic Mechanical Analyzer (DMA) was used to characterize fatigue cracking and evaluate the effects of moisture damage on the Fine Aggregate Matrix (FAM) portion of asphalt mixtures. The FAM specimens should be properly fabricated to represent the composition and structure of the fine portion of the mixture.

The objective of the first phase of this study was to develop a standard test procedure for preparing FAM specimens such that it is representative of the mixture. The method consists of preparing loose full asphalt mixtures and sieving through different sizes. Then, the ignition oven was used to determine the binder content associated with the small size materials (passing on sieve #16). Sieve #16 is used to separate fine aggregates from the coarse aggregates. The applicability of this new method will be evaluated using a number of asphalt mixtures.

The objective of the second phase of this study was to develop software to analyze the data from DMA test. Such software will enable engineers and researchers to perform the complex analysis in very short time. This is Microsoft Windows ® based software, executable in any hardware configuration under this operational system.

DEDICATION

I dedicate this thesis to my parents.

TABLE OF CONTENTS

Page

LIST OF FIGURES

Page

Page

LIST OF TABLES

Page

CHAPTER I
INTRODUCTION

Overview

Asphalt concrete is a composite which consists of two different types of materials: asphalt binder and aggregates. Asphalt binders contain a wide variety of organic molecules, and their chemical compositions vary according to the source of the oil used in their production. Classifying binders in accordance to chemical composition is thus not a simple task, making it easier to use a classification system based on their mechanical performance and physical properties, known as the Superpave binder classification (Roberts *et al.* 1996). Aggregates are generally of mineral origin, varying from hard basaltic rocks to softer eroded river sand. Besides the mineralogical differences, aggregates also differ in size, shape, and texture. For these reasons, each combination of aggregate and asphalt binder results in different performances (Roberts *et al.* 1996, Mindess *et al.* 2003, Huang 2004).

Three main distresses affect asphalt mixes: rutting, low temperature cracking, and fatigue cracking. Each distress can be predicted by distinct methodologies, either theoretical or empirical. However, there is no accurate method to predict the fatigue life of a mix, and results from empirical tests present great variance (Yoder and Witczak 1975, Huang 2004, Papagiannakis and Masad 2008).

A new mechanistic method has been developed to characterize fatigue cracking and moisture susceptibility in asphalt mixes. This test consists of torque applied to a cylindrical specimen of fine aggregate matrix (FAM) by a dynamic mechanical analyzer (DMA). FAMs are a mix of fine aggregates and mastic (mix of asphalt binder and filler, forming a uniform cement paste). While the coarse aggregates are responsible for the interlock and resistance to the compressive loads applied to the asphalt layer, the FAM is what holds the structure together when tensile stresses act on the bottom of the hot mix asphalt (HMA) layer, providing the appropriate cohesion the otherwise granular material would not have.

This thesis follows the style of the *International Journal of Pavement Engineering*.

Two major issues must be addressed when characterizing the fatigue life of asphalt mixes through its FAM fraction. First, in order to create a single, consistent method, applicable in all circumstances, it is necessary to unify the results given by stress- and strain-controlled tests. A model can be adopted enabling the two different test methodologies to be compared to each other by estimating the different amount of energies put into the system. This has been successfully done by Masad *et* al. (2008), Caro *et al*. (2008) and Castelo Branco (2008). The second problem concerns the design of the FAM mix. For any given asphalt mix, one should be able to determine what percentage of the whole asphalt binder used in the full mix actually coats the coarse aggregates as well as the residual percentage that encapsulates the fine aggregate and suspends the filler. In early attempts to determine this percentage, an empirical proportioning between asphalt binder, filler, and fine aggregates was established *a priori*, with this proportion being the same for any mix. Later, another method was created in which an estimation of the film thickness covering each aggregate particle was made, and then, based on the total surface area of each aggregate size, the volume of binder was evaluated. Another method designed FAM specimens based solely on practical results from the laboratory. In this method, one would arbitrarily use an amount (approximately 70%) of the binder used in the full asphalt mix (Kim and Little 2004, Zollinger 2005, Vasconcelos *et al*. 2007, Castelo Branco 2008). All approaches resulted in design failures. Despite the fact each would work for most of the mixes, in some cases, the binder content was either too high, allowing the specimen to creep under its own weight, or too low, resulting in very fragile mixes with high air-void content.

Once samples are produced and the required tests are finished, the data set obtained is ready to be analyzed. This set is susceptible to variations not only in file formatting, but also in the setup parameters chosen for a particular test. These differences result in modifications of the analysis calculation routines already developed throughout the years. Adaptations like these have shown to be time-consuming and unproductive, since they require a good understanding of the mechanic behavior behind the tests. In this sense, the existence of an automated tool (software) that analyzes and gives all required responses to the user without the need of modifications of the calculation steps and with minor interaction with the user has become

necessary. This reasoning diminishes the probability of human error and also eliminates any discrepancies concerning the analyses parameters.

Objectives

As stated above, the unification of a method capable of analyzing data from both stress- and strain-controlled tests has already been developed and has shown to be effective (Masad *et al.* 2008, Caro *et al*. 2008, Castelo Branco 2008). However, some problems persist and they will be the focus of this thesis. In this sense, the main objectives of this work are the following:

(i) Create a new method to design FAM mixes that links it to the original binder content of the full asphalt mix. This methodology should be simple and consistent.

(ii) Develop user-friendly software that allows for the automatic handling of the DMA test data independently of the source of the data or their format. It should also be capable of generating easy to read responses.

Outline of the thesis

This thesis follows the Texas A&M Thesis Manual of March, 2010, and it consists of five chapters organized as follows.

Chapter I is a brief introduction to the problem to be analyzed in the thesis. It also delineates clear objectives that are used to try to solve the problem. Chapter II is a literature review of the analysis of damage in FAM mixtures and how FAM has been designed so far. It also provides the fundamentals for the programming effort. After the previous methods for the design of FAM have been exposed, Chapter III creates a comprehensive description of the new design method. It also includes a section on FAM mix preparation using this methodology and testing of the specimens using the standard DMA test procedure. Chapter IV presents the development of the software for analysis of the data obtained from DMA tests. Information on the architecture and framework of the program is given as well as detailed description of the main structures used in the software code. Chapter V is the final chapter and consists of a conclusion and future research recommendations.

CHAPTER II
LITERATURE REVIEW

Mechanistic analyses of damage in FAM

The use of FAM to assess fatigue life and moisture susceptibility has been shown to be a good method since it overcomes the problem of the heterogeneous composition of the asphalt mix by the analysis of a more homogeneous material (Masad *et al.* 2006a). Moisture susceptibility may be defined as the loss of bond energy between the asphalt binder and the aggregate particles due to the presence of water at the interface (adhesive failure). The presence of water may also lead to the degradation of the binder itself (cohesive failure), but it tends to be overwhelmed by the adhesive failure (Zollinger 2005). Testing the FAM is thus relevant because it is directly linked to crack formation and crack propagation of the full asphalt mix (Kim *et al*. 2003, Masad *et al.* 2006a). The mechanism that drives the phenomenon of crack initiation and propagation is described by different evolution laws (Gdoutos 2005), which become particularly difficult to apply in the heterogeneous media of asphalt mixtures.

The first DMA studies of asphalt mixtures started as early as 1988, according to Masad *et al.* (2006a). However, torsion tests were used for the first time by Kim *et al.* (2003). In this work, three different parameters were used to characterize damage: (i) pseudo-stiffness, (ii) dynamic modulus, and (iii) dissipated strain energy. Fatigue life was defined at a transition point between two inflection points on the shear modulus versus cycles plot, and a fatigue life prediction model based on regression parameters from the experimental tests performed was proposed. In another study, Kim and Little (2003) used the same experimental procedures as in Kim *et al.* (2003), but on a larger scale, and concluded that the addition of filler increased the resistance to micro-cracking.

Zollinger (2005) continued the study, focusing more on the moisture susceptibility of asphalt mixes. In the mentioned work, a fatigue parameter was developed based on the work of Kim *et al.* (2003): the dissipated pseudo-strain energy at a given cycle is divided by the ratio between the dynamic modulus at that cycle and a pre-established reference modulus. This

model has shown to be able to unify results from both stress- and strain-controlled test modes (Masad *et al.* 2008, Caro *et al*. 2008, Castelo Branco 2008) and, thus, is the one used in the analyses of the work here developed.

In this sense, the fatigue life and moisture susceptibility of FAM mixes are evaluated by estimating the amount of energy put into the system necessary to cause damage to a given mix. The computation of the energy values depends on the kind of test performed: stress- or strain-control mode. In controlled-strain tests, a constant displacement is applied to the material at each cycle. This incrementally damages the specimen and, as a consequence, the stress drops throughout the test. In stress-controlled testing, a constant stress level is applied to the specimen, causing incremental damage at every cycle as well. However, in this case, a reduction in the apparent modulus due to the inclusion of damage in the material leads to greater strains and, thus, a definite failure of the sample (Huang 2004, Castelo Branco 2008). On the other hand, the phase angle, described as the lag between load and response of the material (Findley *et al*. 1989), tends to grow in both cases, until a sudden drop in its value is reached (Zollinger 2005, Masad *et al.* 2008, Caro *et al*. 2008, Castelo Branco 2008). This drop is characterized here as the fatigue life of the specimen (Figure 1).

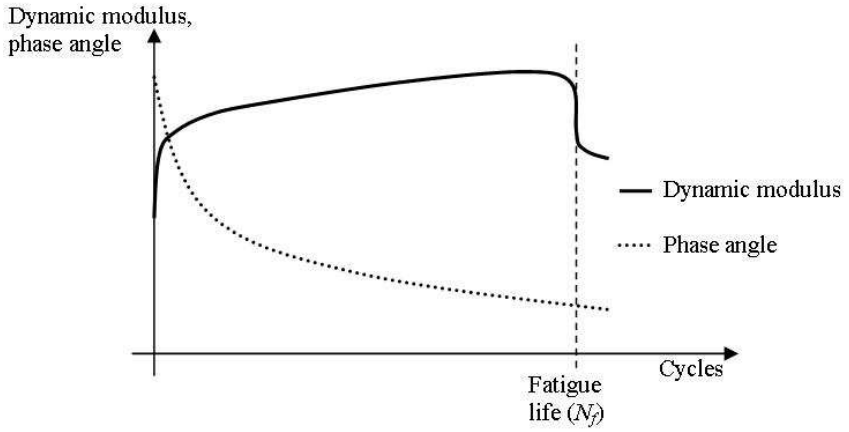

Figure 1: Schematic plot of drop in phase angle value defining number of cycles to failure (fatigue life).

Independent of the type of test, though, the analyses of test results follow similar procedures. As described in Zollinger (2005), for each specimen, two tests must be performed.

The first test is done at a low stress or strain levels. The level is low enough for the material to behave linearly, and thus to infer its linear viscoelastic properties without incurring in changes to the material itself. The second test is run at high stress or strain levels, such that the applied load induces damage in the material. The input load is given in equation (1). (In equations (1) through (10), the first formula represents the strain-control case, whereas the second one represents stress-control).

$$\begin{matrix} \gamma = \gamma_0 \sin(\omega t) \\ \tau = \tau_0 \sin(\omega t) \end{matrix} \quad (1)$$

where γ is strain, τ is stress, ω stands for angular frequency, t is time, and the subscript "0" represents the maximum level (amplitude) of the sinusoidal function. In this sense, the response to the input load for the low strain and low stress test is given by equation (2).

$$\begin{matrix} \tau = \tau_{0,N,VE} \sin\left(\omega t + \delta_{N,VE}\right) \\ \gamma = \gamma_{0,N,VE} \sin(\omega t - \delta_{N,VE}) \end{matrix} \quad (2)$$

In the case of non-linear viscoelastic test with damage, the input load is given by equation (3).

$$\begin{matrix} \gamma = \gamma_{0,F} \sin(\omega t) \\ \tau = \tau_{0,F} \sin(\omega t) \end{matrix} \quad (3)$$

And the response is presented in equation (4).

$$\begin{matrix} \tau = \tau_{0,N,F} \sin\left(\omega t + \delta_{N,F}\right) \\ \gamma = \gamma_{0,N,F} \sin(\omega t - \delta_{N,F}) \end{matrix} \quad (4)$$

where the δ is the phase angle, and the subscript VE stands for linear viscoelastic, N indicates dependency in relation to the number of cycles, and F refers to the test with damage.

Once the input and output are properly characterized, some physical properties can be defined. First, according to Christensen (1982) and Findley *et al*. (1989) we can define dynamic modulus, in shear mode, as presented in equation (5). The formula for stress-control mode is

derived from interconversion relationships between viscoelastic properties in the frequency domain.

$$|G^*| = \frac{\tau_{0,N}}{\gamma_0}$$
$$|G^*| = \frac{\tau_0}{\gamma_{0,N}} \tag{5}$$

From this, Masad *et al*. (2008) define pseudo-strain as:

$$\gamma^R = \frac{|G^*_{VE}|\gamma_{0,F}\sin(\omega t + \delta_{VE})}{G_R}$$
$$\gamma^R = \frac{|G^*_{VE}|\gamma_{0,N,F}\sin(\omega t - \delta_{N,F} + \delta_{VE})}{G_R} \tag{6}$$

where G_R is a reference value for the dynamic modulus. In the present study, this value is chosen as the average of the dynamic modulus during the linear viscoelastic test (i.e., $G_R = |G^*_{VE}|$). However, the notation will be carriedthroughout the derivations below, since there is no unanimity on what G_R should really be.

From this, we define the dissipated pseudo-strain energy (DPSE) as in equation (7).

$$DPSE = \pi\tau_{0,N,F}\frac{\tau_{0,VE}}{G_R}\sin(\delta_{N,F} - \delta_{N,VE}) = \pi\frac{|G^*_{N,F}||G^*_{VE}|\gamma^2_{0,F}}{G_R}\sin(\delta_{N,F} - \delta_{N,VE})$$
$$DPSE = \pi\tau_{0,N,F}\frac{|G^*_{VE}|\gamma_{0,N,F}}{G_R}\sin(\delta_{N,F} - \delta_{N,VE}) = \pi\frac{|G^*_{VE}|\tau^2_{0,F}}{|G^*_{N,F}|G_R}\sin(\delta_{N,F} - \delta_{N,VE}) \tag{7}$$

If the ratio $|G^*_{N,F}|/|G^*_{VE}|$ divides the DPSE, in the case of strain-control test, or multiplies it, in the case of stress-control, we obtain the energy dissipated due to an increase in the apparent phase angle to a given undamaged modulus (W_{R1}), such that:

$$W_{R1} = \pi \frac{|G^*_{VE}|^2 \cdot \gamma^2_{0,F}}{G_R} \sin\left(\delta_{N,F} - \delta_{N,VE}\right)$$
$$W_{R1} = \pi \frac{\tau^2_{0,F}}{G_R} \sin\left(\delta_{N,F} - \delta_{N,VE}\right) \quad (8)$$

Another fraction of the dissipated energy is due to the non-uniformity of energy dissipation within the hysteresis loop, which, itself, is caused by variations of the phase angle throughout the duration of the cycle. For this reason, the value W_{R2} represents the amount of energy not accounted for in W_{R1} and it can be defined as indicated in equation (9) and illustrated by Figure 2. In Figure 2, the inner ellipse represents the hysteresis loop if the phase angle remains the same during the entire cycle, while the outermost plot represents the actual hysteresis loop, which accounts for variations in the phase angle.

$$W_{R2} = \left((\text{Area of stress vs. Pseudo-strain loop}) / \frac{|G^*_{N,F}|}{|G^*_{VE}|} \right) - W_{R1}$$
$$W_{R2} = \left((\text{Area of stress vs. Pseudo-strain loop}) \frac{|G^*_{N,F}|}{|G^*_{VE}|} \right) - W_{R1} \quad (9)$$

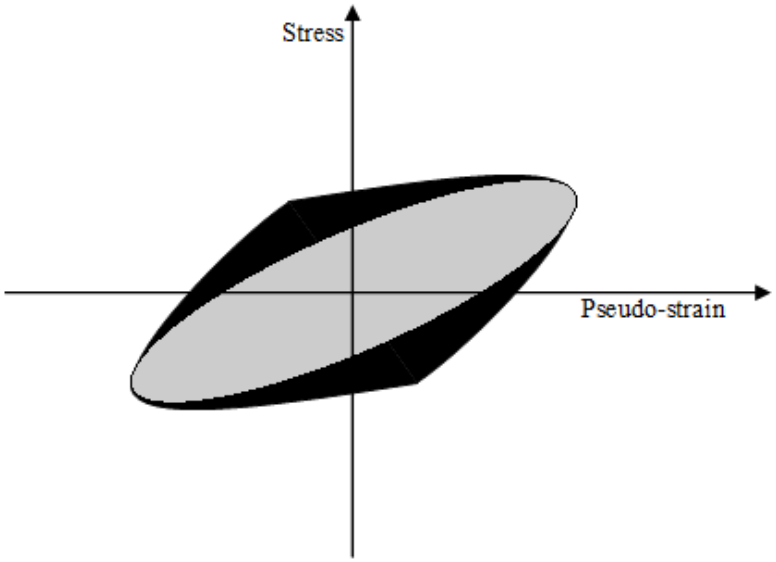

Figure 2: Energy dissipation within a full cycle due to the difference between the real phase angle and the one computed by the DMA.

Furthermore, another component of the dissipated energy during the testing process can be obtained as shown in equation (10), and it is related to the reduction in the pseudo-stiffness (W_{R3}).

$$W_{R3} = \frac{1}{2}\frac{|G^*_{VE}|\gamma^2_{0,F}}{G_R}\left(|G^*_{VE}| - |G^*_{N,F}|\right)$$
$$W_{R3} = \frac{1}{2}\frac{|G^*_{VE}|\tau^2_{0,F}}{G_R}\left(\frac{1}{|G^*_{N,F}|} - \frac{1}{|G^*_{VE}|}\right) \quad (10)$$

A fracture model has been successfully used by Masad *et al*. (2006a, 2006b) and Caro *et al.* (2008). The concept behind it is based on the original work of Schapery (1973), where it is proven that Paris's Law is not an empirical relation between the crack growth ratio as a function of the number of cycles, but rather it is related to the J-integral value. Lytton *et al.* (1993) used the J-integral that quantifies the pseudo-energy release rate per unit crack area (J_R) as given in equation (11).

$$\frac{d\bar{r}}{dN} = A(J_R)^n \tag{11}$$

where $\bar{r}$ is the average crack radius in the sample, N is the number of cycles, A and n are material constants, and J_R is shown in equation (12).

$$J_R = \frac{\partial W_R}{\partial N} \Big/ \frac{\partial (csa)}{\partial N} \tag{12}$$

where csa is the crack specific area and W_R is the dissipated pseudo-strain energy, and it is given as a linear regression from the experimental data by equation (13). The general shape of the dissipated pseudo-strain energy is given in Figure 3. The use of W_R to characterize fatigue cracking properties of FAM or the full asphalt mix allows for the reconciliation of the fatigue life observed by the two test methods. It also makes it possible to differentiate between viscoelastic energy dissipation and energy dissipation by damage, and reduces the high variability associated to fatigue testing (Masad *et al*. 2008).

$$W_R = W_{R1}+W_{R2}+W_{R3} = a + b.ln(N) \quad (13)$$

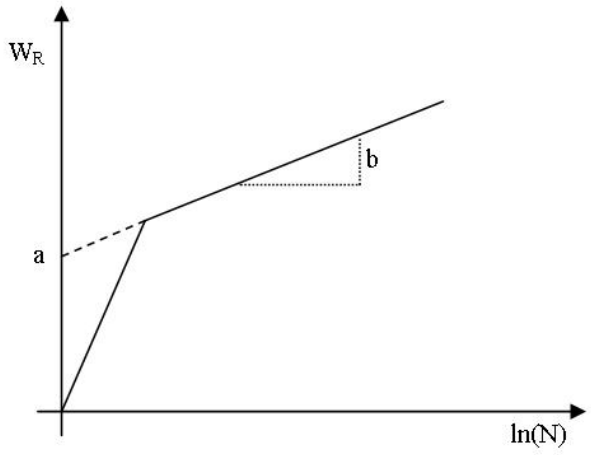

Figure 3: Shape of W_R vs. ln (N).

From equations (11)–(13), it is possible to derive the crack radius index as in equation (14).

$$\Delta R(N) = \left[(2n+1)^{n+1}\left(\frac{G_R b}{4\pi G_1 \Delta G_f}\right)^n N\right]^{1/2n+1} \quad (14)$$

where ΔG_f is the work of adhesion between the asphalt binder and the aggregate. This index grows as the cracks propagate. It can be used to compare the performance of different FAM, as well as moisture resistance for a given mix (Caro *et al.* 2008).

Moreover, the linear viscoelastic relaxation modulus is used to determine the values of G_1 and n from the power law regression curve, as in equation (15).

$$G(t) = G_\infty + G_1 t^{-m} \quad (15)$$

where n is obtained from the relation given by Masad *et al*. (2006b).

$$n = 1 + \frac{1}{m} \tag{16}$$

The work of adhesion is given in equation (17).

$$\Delta G_{f\ (dry)} = \Delta G^{a}$$
$$\Delta G_{f\ (wet)} = \frac{|G_N^*|}{G_R} \Delta G^{132} \tag{17}$$

where ΔG^{a} is the bond energy between the asphalt binder and the aggregate and ΔG^{132} is the bond energy between these same materials, represented by the indexes "1" and "2," respectively, but in the presence of water, which corresponds to the index "3." The detailed formulation on how to calculate ΔG^{a} and ΔG^{132} is given in Bhasin *et al*. (2006).

FAM design methodology

The design of FAM mixes must derive from the original asphalt mix which they should represent. At least two methodologies have been developed to design FAM mixes, and a few variations of these methods were used. In all methods, only aggregates passing sieve number 16 are used. The proportions between these aggregates are kept the same as in the full mix gradation, but they are normalized in relation to largest sieve used (#16), as shown in Figure 4.

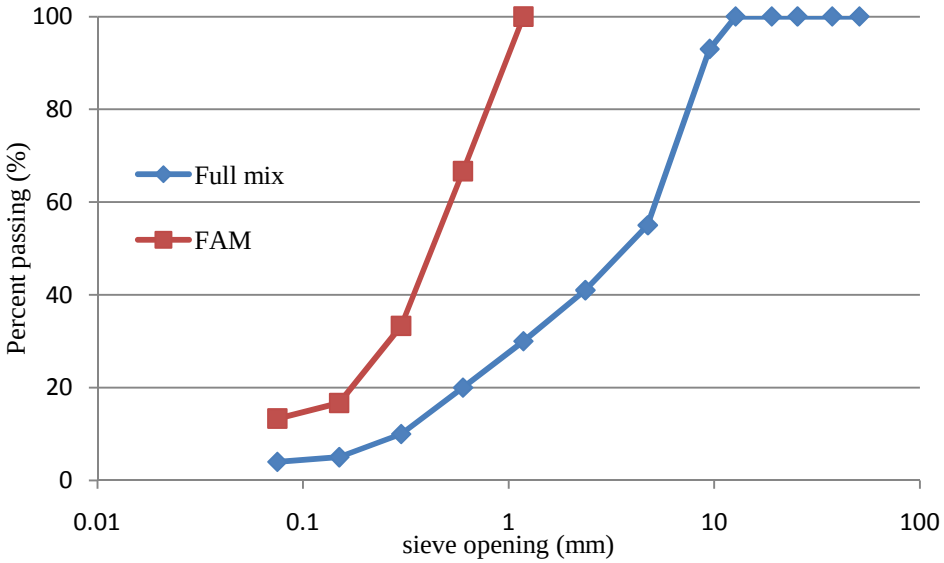

Figure 4: Proportioning of aggregates in FAM.

The methods differ in how the asphalt content is determined. In Kim *et al.* (2003), the binder content is fixed at the same value for every mix. In that work, 8.0% of binder by weight of dry aggregate was used. In Zollinger (2005), this process undergoes a minor change. Instead of proportioning the binder in relation to the material passing sieve #16, the fine aggregates (those passing sieve #16 and retained on #200) are separated from filler (material passing sieve #200). A mixing proportioning of 10:1 between binder and filler produces a mix called mastic, which is then added to the fine aggregates in the same proportion of 8.0% by weight. In this case, the mastic replaces the unmodified binder and the gradation of aggregates is kept proportional just in between sieves #16 and #200. Despite the advantage of creating a repeatable procedure, both these methodologies fail in that they do not create any link between the FAM and the real full asphalt mix. All designs are independent of the aggregate or binder used, thus, no binder/aggregate interactions are considered. Moreover, they do not always result in testable samples. After defining the design, Kim *et al.* (2003) prepared the samples in individual molds where they were individually compacted by a static weight, leading to great variations on the air voids. This method weakness was solved by Zollinger (2005). The author fabricated Superpave Gyratory Compactor (SGC) samples following the standard procedure. From the SGC samples (150 mm diameter by 85 mm height), DMA specimens (12 mm diameter by 50 mm height)

were cut and cored. This new procedure of DMA specimen fabrication allowed for a more uniform distribution of air voids inside the samples and has been adopted in all subsequent work.

A second method is described in Castelo Branco (2008) and has been more widely used. The asphalt content in the FAM is determined in two steps. First, the amount of binder absorbed by the coarse aggregate (following the standard American Association of State Highway and Transportation Officials [AASHTO] T 85; AASHTO 2008a) is subtracted from the total binder content of the full asphalt mix. Then, all the remaining binder is considered to make part of the FAM. Thus, in this situation, the binder content of a FAM is given by weight of non-absorbed binder in the full mix in relation to the weight of the fine aggregates contained in that same full mix. Since not a lot of binder is generally absorbed, the original binder/fine aggregate proportion of the full mix is used in order to simplify the design. Different from the first method, this procedure tries to relate the original mix to the FAM through physical properties of the aggregates and binder. However, designs obtained from this method are not always usable, since it does not result in testable samples.

Object oriented programming and graphical user interface

Most present-day software has a graphical user interface (GUI). In computer science, interface may be defined as the boundary between the user and the functioning part of the system. Many times the user interface (UI) is mistakenly taken as the part responsible for making the appropriate calculations/manipulations asked by the user. In reality, the UI uses metaphors to represent the tasks the system can do (Leventhal and Barnes 2008). The objective of using UIs is to provide subtle clues to the user in such a way that they are easily perceivable. They should also convey the correct message. This property is called, in software development, perceptibility. For an interface to be perceptible, it must offer relevant information allowing the execution of the desired task.

When the UI is associated with graphic and visual resources, it becomes a GUI. This type of UI includes a large variety of resources, commonly known to the every-day user of computers, such as menus and form-filling windows. The use of graphic resources is, thus, of

vital importance to satisfy the principle of perceptibility, making the software "self-explanatory" through the use of so-called widgets (e.g., buttons, check boxes, list boxes, etc.). The choice of widgets reflects the intent of the designer and, for this reason, they must be carefully selected so no dubious interpretations are allowed from the point of view of the user (Stone *et al*. 2005).

Another important factor in software development is the concept of usability. According to the International Standards Organization (ISO), usability is defined as "the effectiveness, efficiency, and satisfaction with which a specified set of users can achieve a specified set of tasks in particular environment" (Mandel 1997, p. 105). While developing software, the designer must consider (i) the type of user, (ii) the type of task to be executed, (iii) the hardware constraints, and (iv) the social/cultural limitations where the software will be inserted. A deep and careful study must be managed to identify these factors. Leventhal and Barnes (2008) state that 80% of maintenance costs are related to unforeseen user needs, whereas only 20% are due to bugs.

Along with the interface, the implementation of tasks is required for the program to be considered useable. Many are the techniques and programming languages that can be used. It is out of the scope of this work to detail the evolution of computing languages, so we will restrict ourselves to expose the choice of structure used.

Given the technological state of development and the use of personal computers in the present days, it is a natural choice to use object-oriented programming (OOP) in this implementation. This kind of paradigm has the advantage of allowing (i) data encapsulation (data hiding) by a class entity and (ii) more natural reuse of code by class inheritance mechanisms (Stroustrup 1997, Prata 2005), resulting in a more elegant and organized source code, easier to expand. Before defining these concepts, though, a better description of classes needs to be done.

The use of OOP literally represents a paradigm shift in programming procedure (it is generally referred to as OOP paradigm, whereas the more traditional method is called procedural programming paradigm). Unlike procedural programming, which focuses on algorithms and their optimization, OOP emphasizes the data. These data are kept together with

functions (or pieces of executable code) in encapsulated sets of logically related items and functions, also known as classes (Stroustrup 1997, Prata 2005, Troelsen 2007, Solis 2008). Classes generally represent objects in the real or conceptual worlds. In this sense, an object is a particular entity built in accordance to predefined structures given by a class. Troelsen (2007) formally defines a class as "an user-defined type that is composed of field data (often called member variables) and members that operate on this data (such as constructors, properties, methods, events, and so forth)." It is beyond the scope of this work to define each concept listed in this definition, but at least two notions must be well established. First, fields, or member variables, are the data stored inside a class. Second, function members, or methods (used here in broader sense than intended by Troelsen) are blocks of executable instructions that can access and/or modify the fields.

Classes can be graphically represented as a box horizontally divided in three parts. Inside the top part, one finds the name of the class. Data members are listed in the middle box and functions in the bottom one. Examples of class representations and of concepts pointed out in the previous paragraph are presented in Figure 5. In this figure, a class called HumanBeing is defined and it intends to represent human individuals by adding to the encapsulated entity factors that the author of the class judge necessary to achieve a complete description. Hence, from what is presented in Figure 5, we could create a person that would be described as an object of the class HumanBeing whose "name" is, for example, John Doe, "height" is 6 ft, "dateOfBirth" is 02/29/1972, and "hairColor" is black. The methods Talk and Think shown in the bottom box would be responsible for making John Doe talk and think, and, when necessary, GetAge would compute the object's (i.e., John Doe's) age at the present date. The casing and naming conventions used in this work follows, in part, that suggested by the C# Language Specification. Table 1, based on the work of Solis (2008), summarizes the used casing.

Table 1: Used identifier naming styles.

Style Name	Description	Use	Examples
Pascal casing	Each word in the identifier is capitalized	Type names and function members	CardDeck, PokerTable
Camel casing	Each word in the identifier, except the first, is capitalized	Local variables, method parameters and data members	totalCycleCount, randomSeedParam
Uppercase	The identifier is composed of all uppercase letters	Abbreviations	IO, DMA

Throughout the execution of a program, some data need to be accessed at different moments. In the procedural paradigm the access to information is somewhat free to happen, leading to data integrity issues. In OOP, data are encapsulated in entities (classes) that restrict access to the data they hold. Three levels of access are granted to any external agent who wants to handle internal data of a class: private, protected, and public. Private data are restricted to methods of a particular class itself. Having this kind of restricted accessibility is an advantage because that specific data will always be handled in a well-known, predefined way, making it easier to protect them against problems such as type-safety or unwanted value change. Access to private data of a class is closed even to classes that inherit from it. This does not happen to protected data. At this level, the data behave just like in the private case, except that derived classes (those that inherited from a base class) have free access to them. The public level allows any entity to access the data inside another class (Stroustrup 1997, Prata 2005, McLaughlin *et al*. 2007, Troelsen 2007, Solis 2008).

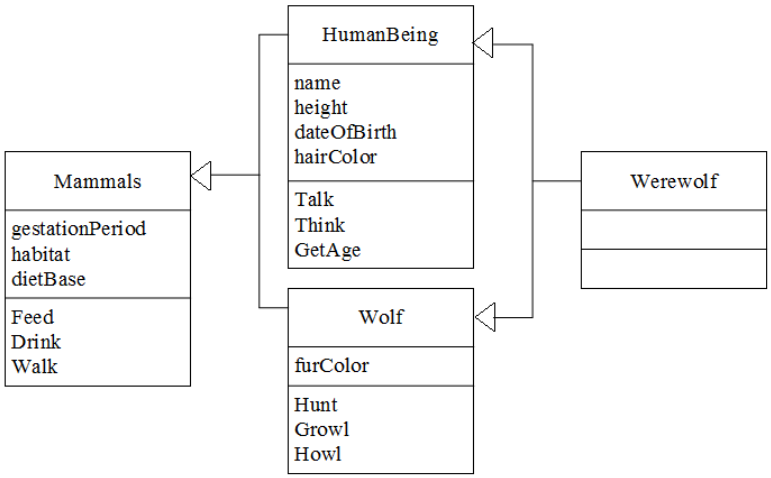

Figure 5: Representation of classes and relationship of inheritance between classes.

As mentioned before, inheritance is a great advantage of OOP. This allows reuse of predefined or preprogrammed blocks in the creation of new classes. It is a simple concept in which a new class inherits the fields and methods of another class as a part of its own. The use of inheritance considerably reduces the amount of written code, making the program more elegant and simpler to look at. In Figure 5, besides the class HumanBeing, the classes Mammals and Wolf are also defined. As a representation of the real world, classes HumanBeing and Wolf inherit from Mammals, incorporating all its members. This means that any object of HumanBeing will carry information not only on the name, height, date of birth, or hair color of the individual, but will also store information on the human gestation period, habitat, and diet base and will keep instructions on how humans feed, drink, and walk. The same is applied to the class Wolf. Another curious and useful feature of inheritance in OOP is the so-called multiple inheritance, where one class can inherit from as many classes as necessary. This is portrayed in Figure 5 by the particular case of diamond inheritance, exemplified by the class Werewolf. Werewolf is noticeable because (i) even if it does not represent a being of the real world, we are still able to define it, (ii) it inherits from two distinct classes, and (iii) it does not have any field or function of its own, being formed solely by the union of the other classes. Diamond inheritance may cause conflicts which are dealt differently by every programming language. Further explanations are out of the scope of this work.

Class diagrams, such as that presented in Figure 5, are a simple way to represent the types of objects and the kinds of relationships existing among them. In Figure 5, the representation of inheritance relation was illustrated by the use of an arrow pointing to the parent class with an empty triangle. This symbol is part of a family of graphical notations that helps in the design and analysis of software systems. These graphical resources are known as the Unified Modeling Language (UML). The UML concept dates from as early as the beginning of the 1990s, but it was only in 1997 that it was officially born (Fowler 2004). UML is complex and can be used as a programming language itself, but, in most cases, it is used only as a sketch to facilitate the creative process (forward engineering) or to explain how some parts of a system work (reverse engineering). A useful concept in UML is the notion of aggregation: an empty rhombus points towards the class that contains a collection of objects of some other class. Figure 6 shows the class WolfPack composed of a collection of objects of the class Wolf.

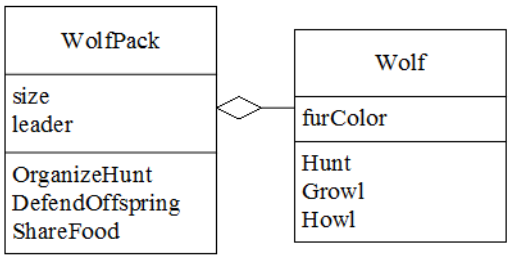

Figure 6: Relationship of aggregation between classes.

CHAPTER III
FAM DESIGN AND TESTING

Introduction

A new method based on a simple, elementary idea has shown to be powerful in yielding consistent results, despite its purely empirical formulation. It was conceived to replace the older methods, making the production of DMA samples consistent and independent of uncertain assumptions. With the intention to compare the results generated from the different methods and to show the efficiency of the new method, the experimental methodology is divided in three parts. The first concerns the determination of the asphalt content of the FAM of four different asphalt mixes by both the old (Castelo Branco 2008) and new methods. The second describes the production of the specimens. The third is related to the results obtained from DMA data analysis. Before comparison, however, descriptions of the new design method, the materials used, and DMA test configuration are presented.

The new design method of FAM mixes

The determination of the binder content is done by isolating the fraction of an asphalt mix that makes part of the FAM. As mentioned before, FAM is the composite formed by asphalt mastic and fine aggregates. Thus, it is imperative to define a limitation to the aggregate size in the FAM mixes. Based on recent research and also on some physical limitations of the DMA equipment, a representative element volume can be obtained by using specimen dimensions of approximately *12* mm (*½* in) diameter by *50* mm (*2* in) height. Still, fine aggregates are defined as those passing sieve #16 (*1.18* mm screen opening) and retained on sieve #200 (*0.075* mm screen opening). In order to estimate the amount of asphalt cement that coats the FAM inside a full asphalt mix, a procedure based on the AASHTO standards T 209 and T 308 (AASHTO 2008b, 2009) was developed and is described as follows.

The first step consists of preparing three samples of the full asphalt mix from which the FAM needs to be determined. The minimum mass for each sample is given in Table 2, as

indicated in AASHTO T 209 (AASHTO 2008b). After mixing, the samples must be subjected to a two hour conditioning period in an oven at *135*°C. This ensures the computation of realistic values for the amount of asphalt absorbed by the aggregate and void properties of the mix (AASHTO 2008b). When taken out of the oven, the mix must be left to cool for approximately half an hour, after which its particles must be separated by hand, as in the procedure used in determining the theoretical maximum specific gravity. This prevents possible fracturing of the aggregates. If it cannot be done at room temperature, the asphalt mix should be warmed in a flat pan until it becomes soft enough to be partitioned by hand. In this case, the sample should be portioned while still warm and spread on a smooth surface where it should be left to cool before putting it on the sieves, as described in the following paragraph.

Table 2: Minimum sample sizes.

Nominal Maximum Aggregate Size (mm)	Minimum Sample Size (g)
≥ *37.5*	*4,000*
19 or *25*	*2,500*
≤ *12.5*	*1,500*

The next step consists of the mechanical separation of the mix particles. The previous manual work is necessary to ensure a larger amount of material obtained for each fraction. For this research, the specimens were screened at room temperature through sieves #4, #8, and #16 by mechanical agitation. In each sieve, 9.5 mm stainless steel balls (from the micro-deval apparatus – AASHTO T 327 [AASHTO 2006]) were used in the respective amounts of 40, 30 and 20 balls (Figure 7) in the mentioned sieves. Sieving the mix while hot was tried, but it resulted in less material passing sieve #16 and in clogging of the screens, so it is not recommended. Figure 8 shows two samples after the screening process is completed. After the screening process is completed, the four fractions obtained were separated into different groups, organized as follows:

- Group 01: material retained on sieve #4,
- Group 02: passing sieve #4 and retained on #8,
- Group 03: passing sieve #8 and retained on #16, and
- Group 04: passing sieve #16.

(a)

(b)

Figure 7: (a) Loose sample on the right, before being sieved through the set of sieves on the left, equipped with stainless steel balls. (b) Mechanical sieving being performed.

Figure 8: Two samples after sieving is completed. Four fractions are obtained for each sample.

The materials from the different groups were kept separated from each other and individually submitted to the next step, which is based on AASHTO T 308 (AASHTO 2009). This standard describes the verification of the asphalt binder content in a full asphalt mix by the use of an ignition oven. These ovens reach temperatures (500°C) far above the flashpoint of binders (200°–250°C), making it burn (ignite) and leaving behind only the aggregates. The use of the ignition oven does not lead to thermal decomposition of limestone ($CaCO_3$) into

quicklime (CaO) and carbon dioxide (CO_2), since this reaction takes place at temperatures close to 900°C (Mindess *et al*. 2003).

AASHTO (2009) standard also specifies the minimum amount of material to be ignited based on the nominal maximum aggregate size (NMAS). Among all different fractions studied, though, only group 01 (retained on sieve #4) actually had a known NMAS (the same as the full mix). In addition, because it was not possible to predict the correct amount of asphalt mix retained on sieve #4, the values specified in AASHTO T 308 could not always be followed. Indeed, these values have shown to be impractical due to the large amount of asphalt mix necessary to attend the specifications in some cases. Despite the fact that the standard was not followed, no shortcomings were found, and the final results were very consistent, as is shown.

Each fraction should be oven dried to a constant mass at a temperature of *110*°C. After that, the basket/catch pan system designed for the furnace is weighed (W_p) and the dried material is transferred to it, which is then weighed again (W_M), as in Figure 9a. The scales used for groups 01, 02, and 03 have a resolution of *0.1* g. In the case of group 04, the whole procedure had to be revisited due to the small amount of material obtained. First, a scale resolution of *0.1* g was not appropriate and, thus, a more precise one was used, with a resolution of *0.001* g. Because scales with this kind of precision have a low limit on the mass they can measure (approximately *150* g), the original basket/catch pan system could not be used, since they exceed this limit. The material was therefore put into pressure aging vessel (PAV) pans (Figure 9b), which are sufficiently small to be within the limits of the scales (even with material on them) and big enough to accommodate all the material at once. In addition, these pans can resist the high temperatures of the furnace. Another advantage of using the PAV pans is that their dimensions allow three samples to be tested in the oven at the same time, making the process energy- and time-efficient. For these pans to be properly put in the oven, the catch pan was used, as shown in Figure 9b. it is important to emphasize that each fraction group is taken to the ignition oven separately and the basket/catch pan system is cleaned at the end of each test. The fact that the PAV pans with group 04 material are on the catch pan does not mean they were taken to the furnace at the same time as some other group: the catch pan is made necessary because the supporting system inside the oven could not properly hold the PAV pans.

(a)

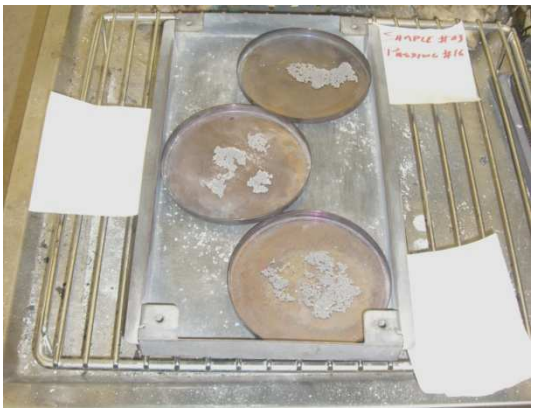

(b)

Figure 9: (a) Material retained on #04 placed on a dual basket/catch pan system before burning in the ignition oven and (b) three PAV pans inside the ignition oven catching pan after burning.

Burning is considered complete after 3 minutes with no change in mass superior to 0.01%. A minimum limit of 10 minutes is also required. After the burning cycle is completed, the pan and baskets are removed from the furnace and placed over a cooling plate or block, where they rest for approximately 30 minutes, properly covered with a protective cage. When cooled, the pan and burnt material are weighed again and the value is noted as W_A. The binder content in each group is calculated by equation (18) below.

$$P_b = \frac{W_M - W_A}{W_M - W_p} \times 100\% \tag{18}$$

Additionally, as a verification of the accuracy of the method, a back-calculation of the binder content in the full mix is done as indicated in equation (19), and the result compared to the design value.

$$P_{b-mix} = \sum_{i=1}^{4} \left[\left(W_{M_i} - W_{A_i} \right) \times P_{b_i} \right] \quad (19)$$

Materials

The materials used to develop the new design method for FAM mixes were carefully chosen to represent the main different kinds of aggregates found in asphalt mixes. For this reason, three distinct mixes, each composed exclusively by one type of material, were chosen. These mixes are identified by the material of which they are composed: granite, gravel, and limestone. A fourth kind of mixture was also chosen, this one composed mainly of limestone and crushed gravel as aggregates, but whose main purpose is to test the new method in a mix where the older methods had failed. Due to the fact that it was a mix used in the state of Texas, the specimens of this mix were identified by the state's name. A summary of the four different mixes, their materials composition, and used binders are given in Table 3.

Table 3: Mix compositions.

Mix type	Material passing sieve #16 (%)	Material passing sieve #200 (%)		Binder	Material origin
		In relation to the full mix	In relation to the FAM mix		
Limestone	26.0	6.14	23.6	PG 70-22C	Sabinal/Knippa, TX
Granite	27.0	5.1 (2% lime)	18.9	PG 70-28	Childress, TX
Gravel	30.8	4.0 (1% lime)	13.0	PG 64-22S	Fordyce, TX
Texas	26.1	2.75	10.5	PG 76-22	Freer, TX

All mixes were initially prepared in a 100 mm cylindrical Superpave Gyratory Compactor (SGC) mold and then cored using a coring bit refrigerated by water. For each mix type, two SGC samples were produced, one for each design method. From these SGC samples, DMA samples were cored, allowing testing at dry and wet conditions (three specimens for each case, when extraction was possible). Table 4 summarizes the types of specimens produced, showing the names attributed to each sample kind.

Table 4: Specimen type names given by materials used and test conditions.

Specimen type	Test condition			
	Dry		Wet	
	Old method	New Method	Old method	New Method
Limestone	LsOD	LsND	-	LsNW
Granite[a]	GtOD	GtND	-	GtNW
Gravel	GvOD	GvND	GvOW	GvNW
Texas[b]	-	TxND	-	TxNW

a: Only one sample could be obtained for the old method.

b: Specimens for the old method were not obtained because the SGC samples could not be cored.

Test configuration

DMA testing consists of a torque applied in the same direction of the sample axis. The torque necessary to perform the test may be very high, depending on the sample stiffness, and thus one must be concerned with the limitations of the used machine. The new design of FAM delivers rather rigid specimens, making this a major issue to be avoided. In this sense, the test temperature needs to be raised to 30°C, since it is warm enough to render the specimens softer and testable. Strain-controlled tests were chosen to be performed on all samples.

The test is performed in four different stages. The first stage is to raise the environmental chamber to the target temperature and to have it stabilize for a pre-determined period. Once the specimens' dimensions are not very thick and the difference between room and target temperatures is roughly *5*°C, it was assumed *20* minutes to be a time long enough for the sample core to reach *30*°C. The second step is the relaxation modulus test. This test is run at a very low strain (6.5×10^{-3}%), which is applied to the material for 10 minutes. The third step consists of a cyclic load in the linear viscoelastic domain of the FAM mix. Even if no testing is made to find the linear viscoelastic limits of the material being tested, the strain of 6.5×10^{-3}% is small enough, making it a reasonable assumption. This step takes only two minutes, enough to reach a steady state. The final step is also a cyclic test, but now with a higher strain of *0.35*%. This strain is high enough to assure that the non-linear viscoelastic region has been reached. The constitutive equation used to model the experiment can also account for damage; thus one need not worry with the actual effects of this stipulated strain. Moreover, it is also important to point out that the last step is set to take up to four hours, being interrupted if specimen failure is reached before. The last two steps are performed at o Hz.

Experimental setup

The tests started with the determination of the asphalt content for the mixes. The old (as described in Vasconcelos *et al*. 2007, Castelo Branco 2008, Caro *et al*. 2008) and the new methods were carried out and their results are presented in Table 5. SGC samples were produced for both methodologies with the intent to prove the efficiency of the new method in giving consistent values.

Table 5: Comparison between different asphalt contents of FAMs obtained using different methodologies. The percentages are given by weight of mix.

Mix	Binder content (%)		
	Old method	New method	Original design
Limestone	10.7	8.0	4.5
Granite	12.0	7.0	5.3
Gravel	8.9	7.8	4.3
Texas	15.9	8.6	4.7

As pointed out before, the minimum value recommended by AASHTO T 308 could not always be achieved. The non-compliance to the standard requirements did not yield bad results, as indicated in Table 6. In fact, the back-calculated asphalt binder (equation (19)) content of the mixes was very close to the design value, with a maximum absolute difference of 0.43% or a 9.6% relative difference. It should also be noted that the binder content obtained for each fraction group presented very consistent results. Their averages are shown in Table 6. The maximum standard deviation is of 0.34% among all groups and 0.24% within group 04 alone. Figure 10 exemplifies how consistent the results were and also provides an idea on how the asphalt binder is distributed according to the different sizes of aggregates.

Table 6: Asphalt content of mixes fractions groups and comparison between the back-calculated binder content and the original binder content of the mixes. All values are in percentage (%) by weight of mix.

Fraction groups	Binder content (%)				
	Limestone	Granite (1)	Granite (2)	Gravel	Texas
01	3.81	4.35	4.47	3.48	4.13
02	6.69	5.99	5.93	5.82	6.60
03	7.37	6.57	6.54	7.80	8.06
04	8.00	6.97	-	7.28	8.65
Original design P_{b-mix}	4.5	5.3	5.3	4.3	4.7
Back-calculated P_{b-mix}	4.93	4.88	-	4.37	4.91

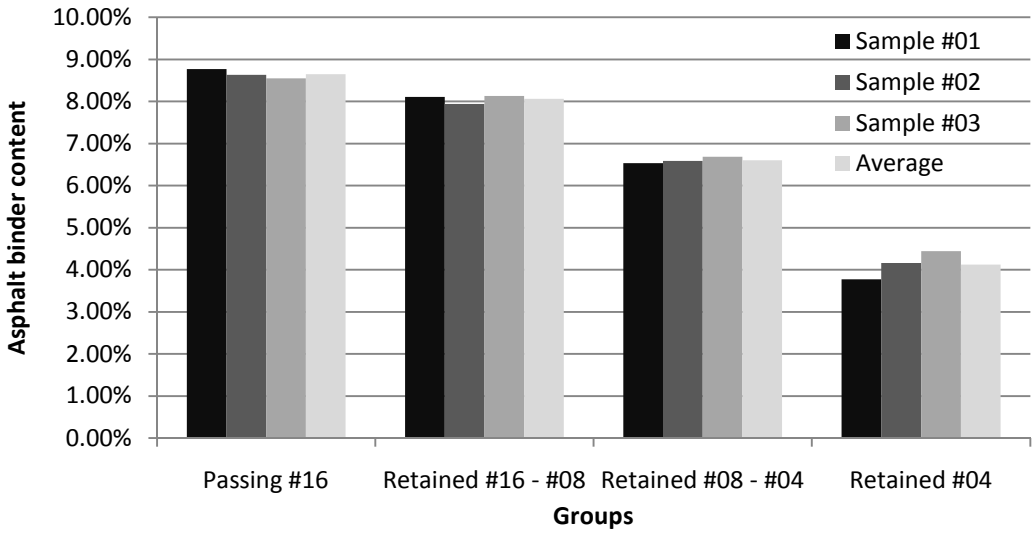

Figure 10: Detailed information about the asphalt contents of each fraction group for three different samples and their averages (Texas mix).

Despite all the available data, it was decided that the binder content given by the material passing sieve #16 sufficed to the design of the FAM mixes. Figure 11 shows the aspect of the material from group 04 before and after the burning process in the furnace. Simpler sieving can be performed by separating the full asphalt mix in only two fractions, which will give the same results. The separation into more fractions, though, is recommended for a series of reasons: (i) it is useful as a verification of the repeatability of the test, (ii) it will contribute to the compilation of an empirical database that may allow further studies on the distribution of film thicknesses and particle interactions, and (iii) it results in a greater amount of material

passing sieve #16. In this sense, , it is recommended that at least on more sieve (#8) be adopted in addition to #16.

Furthermore, the importance of having data for different sieves is illustrated by the gravel mix. Group 03 of this mix has a higher binder percentage than group 04, which does not seem logical at first. For this reason, every group of every mix was sieved through the same set of sieves after having been submitted to the ignition oven. This sieve analysis of the gravel mix shows that a large amount of aggregates and filler passing sieve #16 is present in group 03. Indeed, the amount of material passing sieve #16 in group 03 after ignition is *2.4* times greater (in mass) then the material passing #8 and retained in #16 for the same group, after ignition. This value varied between *0.8* and *1.3* for the other three mixes. Thus, the high asphalt content of group 03 in the gravel mix can be justified by the presence of a large amount of fine particles, a fact that disturbed the average in that group. This also led to a change in the design of the FAM. The binder content for the gravel FAM adopted was that of the group 03, instead of the one found for group 04. This choice was made because the large amount of material passing sieve #16 compared to that retained by it for that group portrays in a better way how the mastic coats the aggregate particles.

(a)

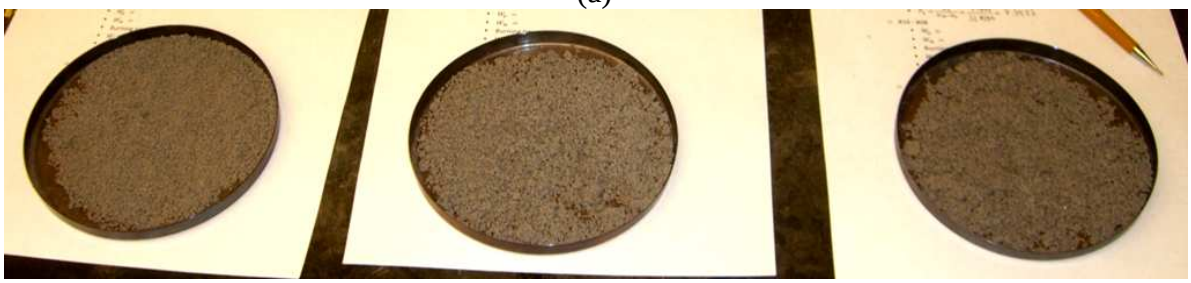

(b)

Figure 11: Group 04 fraction (a) before and (b) after ignition oven test.

FAM mixing and coring

After the design proportions had been defined, it was time to mix and prepare the FAM samples on the SGC. All batches were mixed and compacted successfully. The limestone sample with 10.7% binder (old method) crept under its own weight, as shown in Figure 12.

Figure 12: Two limestone SGC specimens prepared with different asphalt contents. The one on the right has crept under its own weight, resulting in a slight “barrel” shape.

The next step consists of the extraction of DMA samples by coring. Once again, the new method has shown to be more efficient, allowing samples to be extracted for all mixes. For the old method, only the granite sample could have DMA specimens extracted. All other extracted cores presented a visually poor surface due to changes suffered in the binder structure after exposure to high temperatures in the coring process. The limestone SGC sample obtained with the old method could be cored too, but demanded experience from the operator of the coring-machine not to fracture or overheat the samples and was time-consuming.

DMA test results

The final step is the DMA test itself. As indicated in Table 4 and described in the previous paragraph, not all specimens could be tested. In addition, it was chosen not to test the old method specimens for all mixes after moisture conditioning, since the main purpose of the work is not to compare the performance of the methods in fatigue/moisture susceptibility tests, but rather to show that the new method results in testable specimens for any possible study case. The results from the tests of the different mixes are presented in Table 7, in which the columns are the parameters of equation (14).

Table 7: Parameters obtained from the DMA tests to compute the crack radius index.

Mix	Condition	Method	b (J)	G_R (Pa)	G_1 (Pa)	m	n	ΔG_f (J/m^2)
Limestone	Dry	New	*362.93*	*9.08E+08*	*1.31E+08*	*0.42970*	*3.327212*	*0.09705*
		Old	*177.94*	*2.83E+08*	*3.74E+07*	*0.50521*	*2.979396*	*0.09705*
	Wet	New	*1357.17*	*8.87E+08*	*2.34E+08*	*0.38123*	*3.623102*	*-0.1482*
		Old	-	-	-	-	-	*-0.1482*
Granite	Dry	New	*1062.02*	*5.43E+08*	*6.85E+07*	*0.38900*	*3.567704*	*0.1087*
		Old	-	-	-	-	-	-
	Wet	New	*448.91*	*6.95E+08*	*1.03E+08*	*0.40342*	*3.478785*	*-0.1754*
		Old	-	-	-	-	-	-
Gravel	Dry	New	*1252.94*	*7.96E+08*	*1.43E+08*	*0.33557*	*3.980039*	*0.1272*
		Old	*1487.45*	*1.45E+09*	*3.83E+08*	*0.25633*	*4.901286*	*0.1272*
	Wet	New	*1047.26*	*6.93E+08*	*2.65E+08*	*0.28891*	*4.461296*	*-0.1605*
		Old	*1808.40*	*1.30E+09*	*5.32E+08*	*0.27473*	*4.639955*	*-0.1605*
Texas	Dry	New	*1773.78*	*1.13E+09*	*2.76E+08*	*0.29735*	*4.36303*	*0.1138*
		Old	-	-	-	-	-	-
	Wet	New	*1817.92*	*8.32E+08*	*5.03E+08*	*0.38204*	*3.617547*	*-0.1878*
		Old	-	-	-	-	-	-

From the parameters given by Table 7 and using the data obtained in the non-linear cyclic strain-controlled test, the bond energy degradation in the presence of water can be calculated (Figure 13). With that information, the crack growth in the asphalt mixtures may be predicted for both the wet and dry conditions according to equation (14) and which results are plotted in Figure 14 and Figure 15. The plots corresponding to the Texas mixture are not presented at this moment, since they make part of a more detailed study, which is exposed in the paragraphs following Figure 15.

As mentioned before, all mixes were prepared with both old and new methods, but not all specimens obtained with the old method could be tested. Thus, a full comparison could only be obtained for the gravel and limestone mixes. For the limestone mix, the moisture susceptibility of the FAM obtained with the new method is noticeably greater than that given by the old method, regardless of the fact that the crack radius indexes for the dry mixes are essentially equal for both methods. In this sense, while the difference in $\Delta R(N = 5{,}000)$ between the dry mixes is 9.67%, this difference increases to 120% for moisture-conditioned

specimens. It is important to note, however, that some of the new method FAM samples reached complete failure in a very small time. No bad consequences resulted from it, but, in other cases, it may lead to great variability in the data. In this scenario, it is recommended to use a lower strain level for the high-strain test step. For the gravel mix, the moisture susceptibility of the old method is already very significant; thus no difference can be noticed. In general, moisture susceptibility of the new method has shown to be more accentuated. This is mainly due to a smaller amount of asphalt coating the aggregates and a higher porous media, allowing water diffusion.

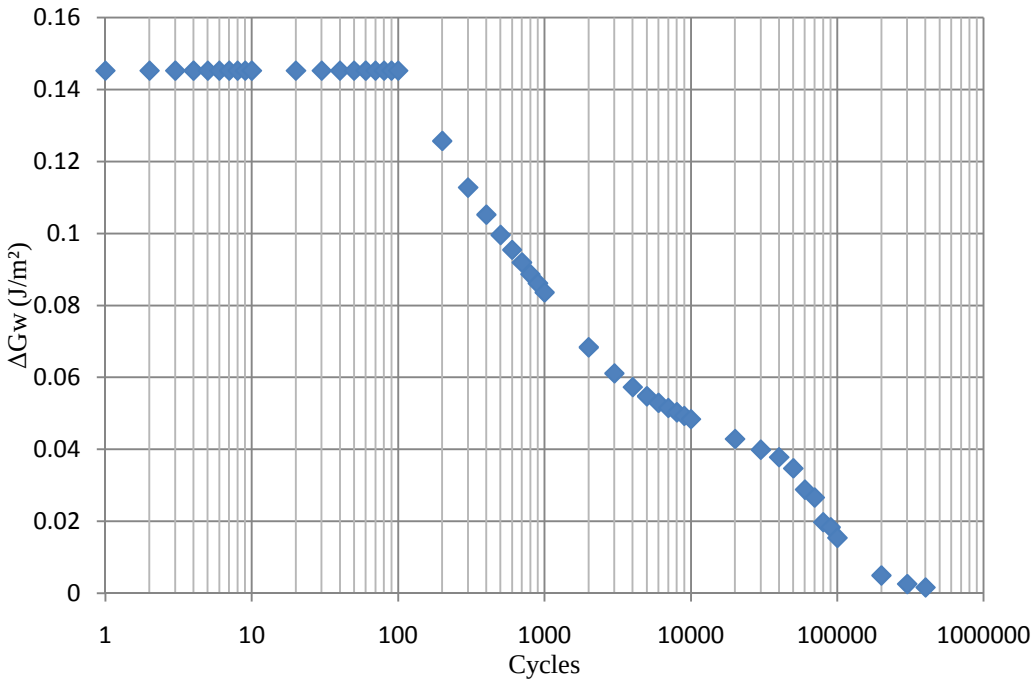

Figure 13: Surface energy bond between granite and asphalt binder in the presence of water.

As it would be expected, the old method delivers better quality specimens when it comes to crack formation and propagation. This is a consequence of the higher binder content, allowing for a more uniform (fewer initial voids) media and a higher rate of healing.

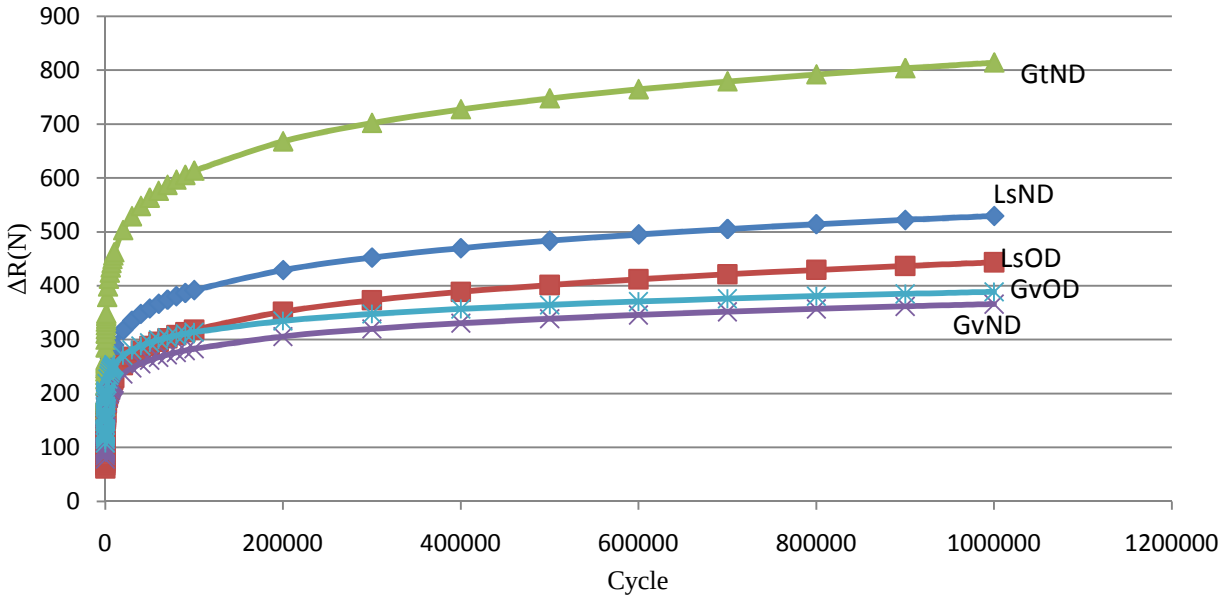

(a)

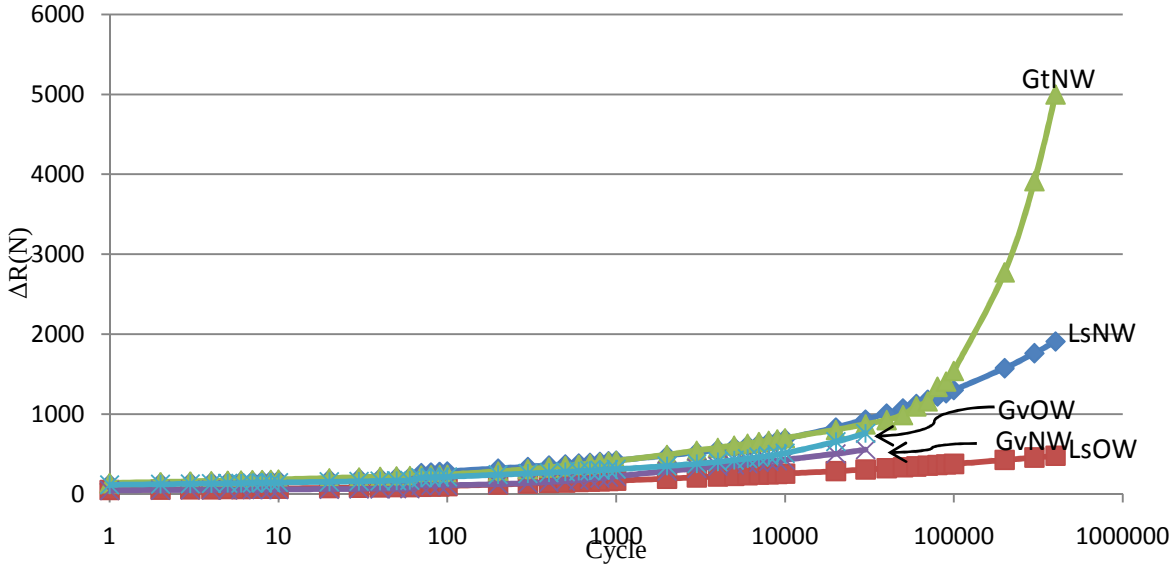

(b)

Figure 14: Performance of (a) dry and (b) wet mixes for both new and old methods. (b) is plotted against Log(N) due to the high sensibility of gravel and Texas mixes to the presence of water.

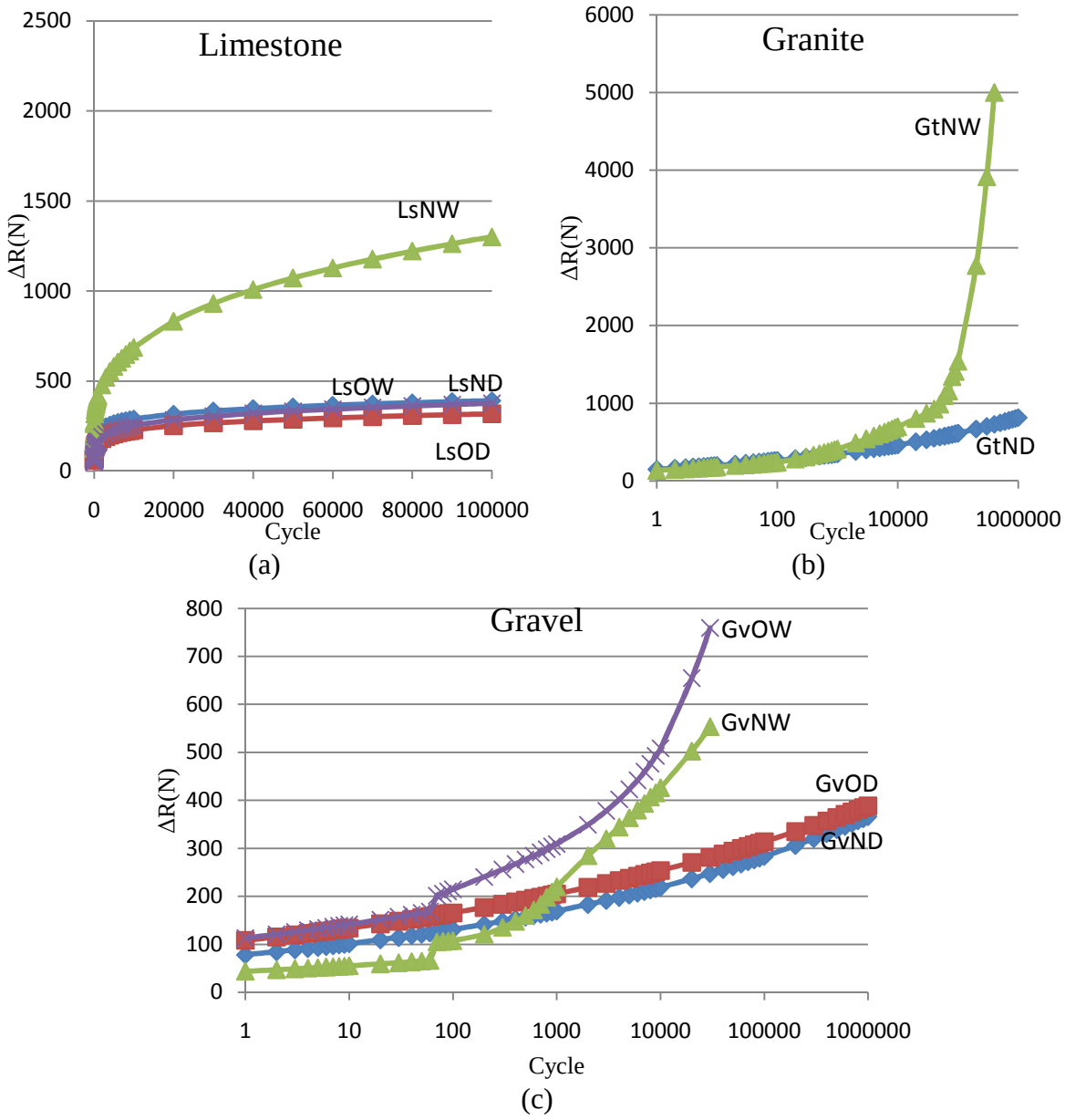

Figure 15: Crack radius indexes of three different mixes: (a) limestone, (b) granite, (c) gravel.

Another set of experiments was performed in order to study the impact of the use of binder modifier and the presence of lime in the mixture. For this specific analysis, the Texas mix was chosen because it had made part of a previous laboratory study where indirect tensile tests were performed for the full mix. The Texas mix has three different designs: the first being the control mix (which the data for crack radius index calculations are presented in Table 7), a

second with the use of anti-strip liquid, and a third with the use of 1% lime in replacement of the fines. The performances of the analysis are presented in Figure 16. This figure shows that the performances of the samples are distinct, reflecting the different characteristics of the interaction between binder, aggregate, and additive. The results of the crack growth index partially reflect the result from the moisture susceptibility obtained from the full mix, as presented in Table 8.

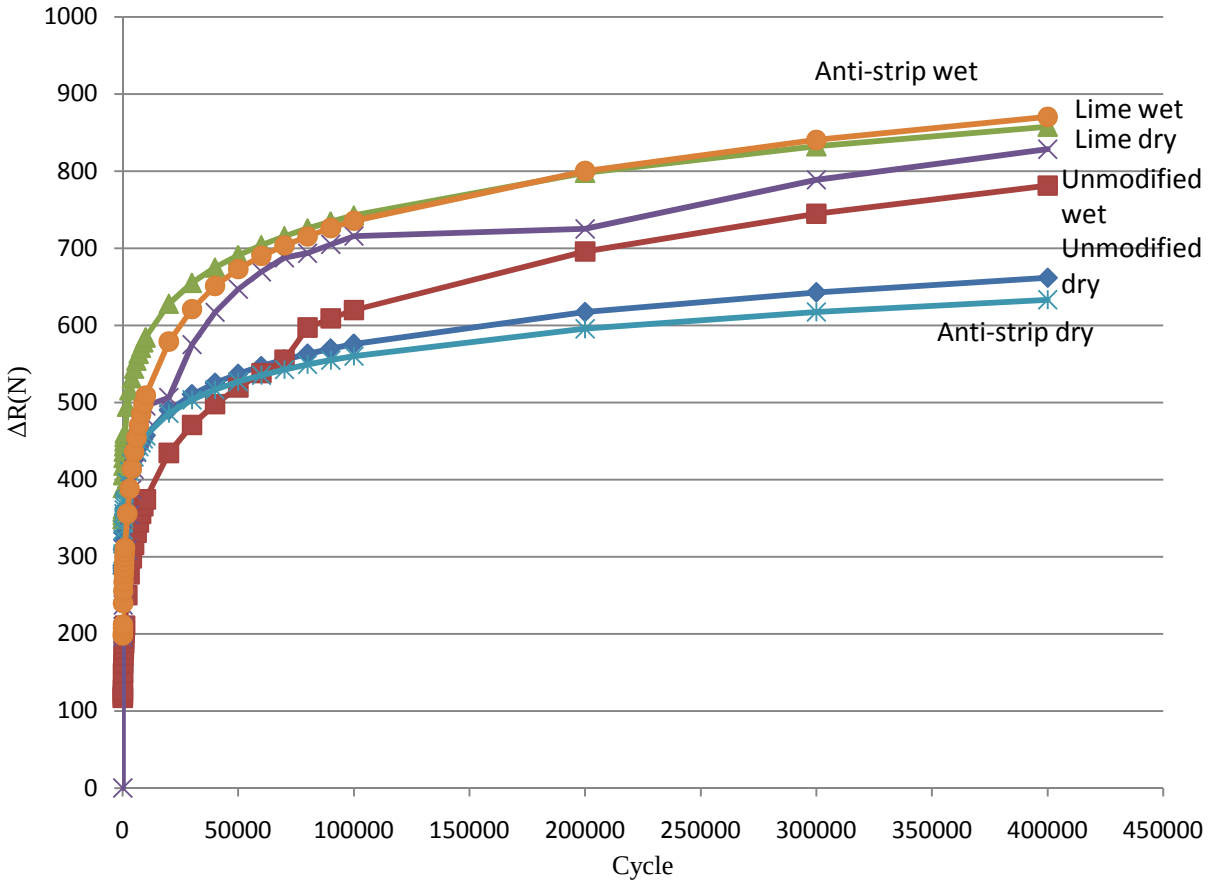

Figure 16: Crack radius index for all three Texas mixes variations in both dry and wet conditions.

Table 8: Comparison between laboratory performances of the full mix and the FAM.

	Test	Untreated	Liquid treated	Lime-treated
Indirect tensile	Dry condition, psi	159	112	155
	Wet condition, psi	98	112	153
	Tensile Strength Ratio, %	61	100	98
DMA	Crack radius index (dry)	661.5	857.5	633.2
	Crack radius index (wet)	781.1	857.7	870.1
	Ratio at 400,000 cycles (%)	84.7	100	72.8

CHAPTER IV
SOFTWARE DEVELOPMENT

Introduction

The software is structured in three different modules that were developed separately. The programming language chosen is C# (pronounced “see sharp”), which is conceived to work in Microsoft’s .NET environment. Many reasons lead to this decision, such as its similarity to C++ (a widespread language used worldwide) and its object-oriented framework. It also results in a consistent and elegant program, with an extensive library and resources both for computing and calculation, as well as for visual resources. Besides these, the Microsoft .NET framework includes important features, as indicated by Solis (2008). The language supports different platforms, meaning it can be executed on different computers, from desktops to personal digital assistants (PDAs), and even cell phones. Furthermore, it is very secure, providing a safe execution environment. Another fundamental characteristic of the C# language is its inherent interoperability with Microsoft Office products. Since many computers run on operational systems and office tools from Microsoft, C# became a natural choice. Yet another reason to justify the use of C# is its capacity to implement asynchronous program execution, or multithreading, which enhances the efficiency of the final software, especially since multi-core processors are becoming standard in new machines.

Program overview

In the analysis of DMA data, there are different levels of complexities, which will be treated according to the user’s necessity and/or availability of data. For this reason, the development of the software was divided into three main modules that are summarized in the following sections.

Level 01A – partial result

A GUI asks the user to load the files to be analyzed. The user loads all the files related to one given mix design at this time. All files loaded are read and handled together. A spreadsheet will be generated in Microsoft Excel for each file entered; however, the overall result will be based on an average.

The input file can either be in text (.txt) or in Microsoft Excel (.xls and .xlsx) format, as shown in Figure 17a. After the data set is loaded, the user must give some general information about the test procedure used (Figure 17b) and, after this, all calculations are done automatically. The main results from this module are the dissipated pseudo-strain energy and the regression parameters a and b from equation (13). Figure 18 presents the output file resulting from the data loaded in Figure 17a for the program execution at Level 01A. Observe that, as indicated, five files were analyzed, corresponding to the first five sets of columns shown in the plot, plus one extra set is inserted, corresponding to the average result.

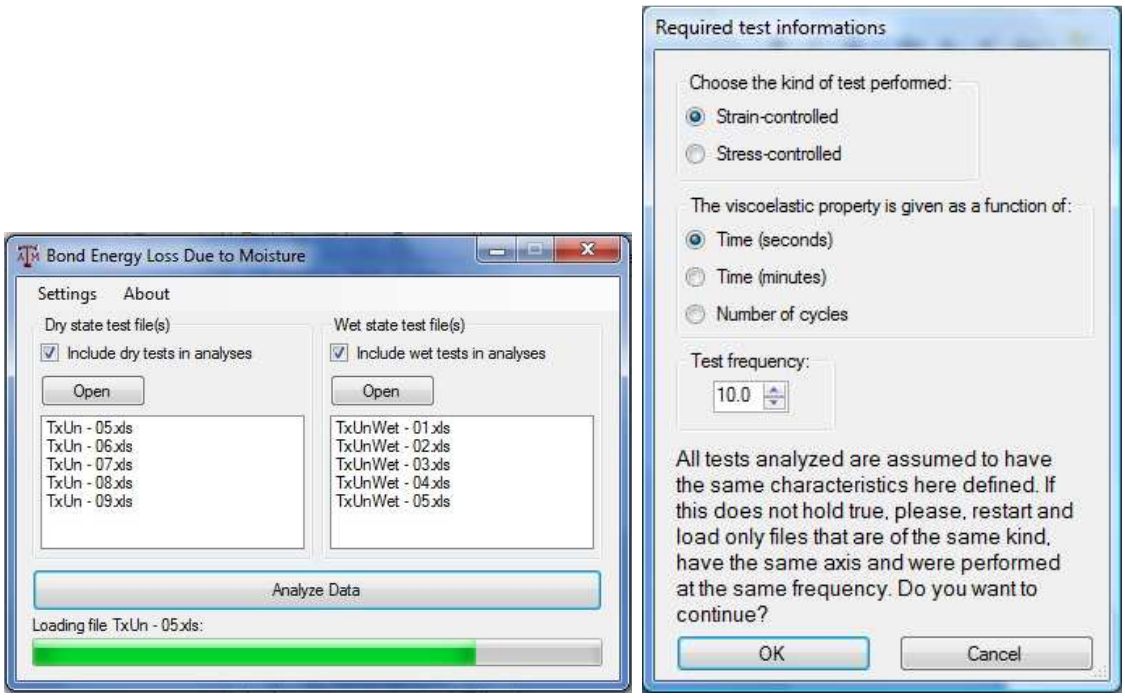

(a) (b)

Figure 17: User interface and files input.

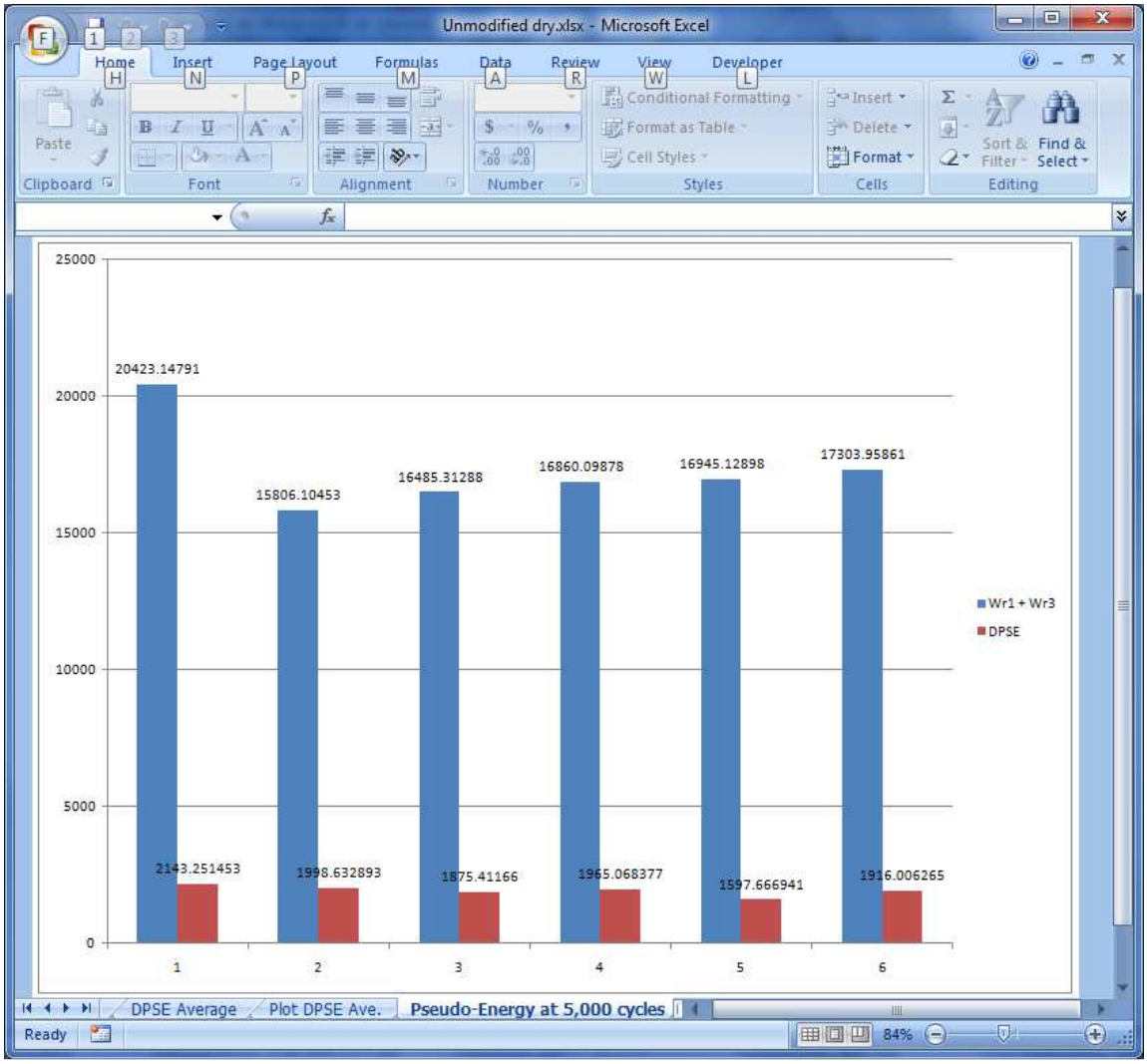

Figure 18: Example of an output file generated after conclusion of Level 01A.

Level 01B – total result

This module includes one extra calculation step to be added to Level 01A. It was observed that not all DMA equipment used rendered available the necessary data to compute the total dissipated energy from the tests. To account for the energy lost due to permanent deformation caused during the load/unload cycles (W_{R2}), detailed information about the stress-strain history during the cycles is necessary. If these data are accessible, they must be given in a separate file, as shown in Figure 19.

Due to the fact that it is not possible to predict file formats, this is the only step of the software where a file configuration is imposed upon the user. If the user is working with Excel files, he or she must have one spreadsheet for each reported cycle, with that sheet being identified by the number of the cycle for which it holds information. The text file must have all reported cycles organized in chronological order, and each one should be properly identified with the cycle number preceding the data alone in one line. In both file formats, data must be organized in such a fashion that the stress column is always the first, followed by the strain column.

If data points are not collected evenly throughout a cycle, an extra column must be included designating at what moment a certain point was acquired. If a third column is not given, the software will assume all points composing a cycle were taken at a constant ratio through the duration of the cycle. It is also possible that the DMA makes the phase angle available for every acquired point. Since this information is not useful for calculations, it must be excluded from the file.

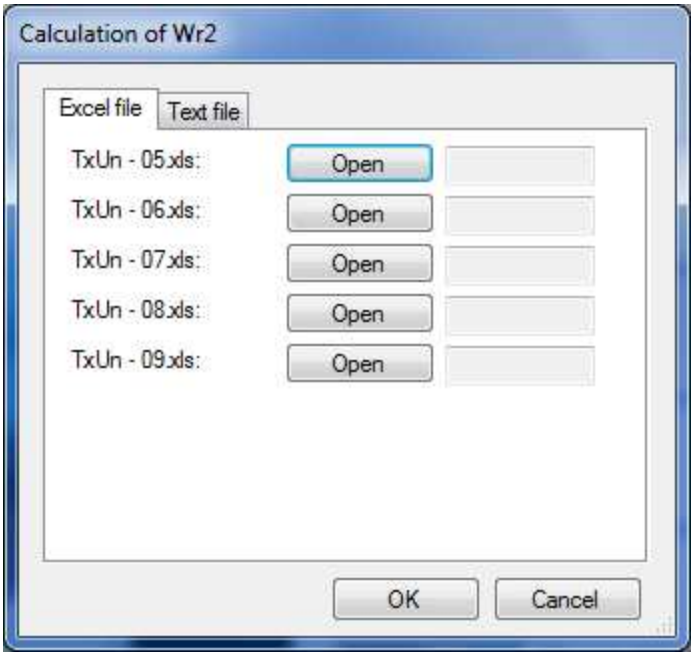

Figure 19: Popup window responsible for loading W_{R2} files.

Level 02

The second level can only be executed if the user has data available on the surface energies of the aggregates and asphalt binder. This level of analysis is executed after Level 01 if the user chooses so in the settings menu. Similar to what happens in Level 01, this level is also divided into cases “A” and “B,” with the same meaning as before, that is, if Level 02B is demanded the W_{R2} calculation step will be called, as in Figure 19. The default analysis will call for the execution of this module in mode “A.” The selection of execution mode is shown in Figure 20.

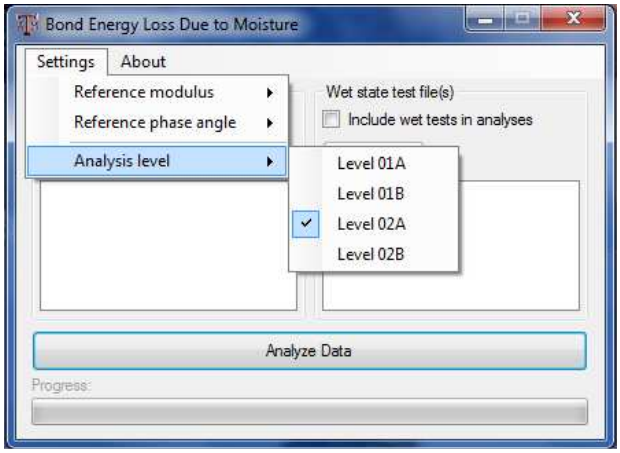

Figure 20: Selection of level analysis.

The program calculates the bond energy between the aggregate and binder and compares the performances between dry and wet states. This analysis infers the work of adhesion ΔG_f. A simple curve fitting of a relaxation modulus test to the equation (15) is performed as well. With the parameters obtained from these steps, it is possible to calculate the crack radius index as given in equation (14).

Independent of the level of analysis chosen, an output file based on Microsoft Excel is generated. The output file consists of multiple sheets where the results of each sample are shown and plotted. One extra sheet is created with the average of all samples for both Levels 01A and 01B. As for Level 02, spreadsheets with the values of the bond energy in dry state, as well as the bond energy degradation in wet conditioning, are presented. The crack radius index plot is the last sheet shown in the file. The values are calculated based on the averaged data obtained from Level 01.

Program architecture

The architecture of the program is presented in Figure 21, where Levels 01 and 02 are emphasized by the dashed boxes. Modes “A” and “B” are not differentiated in this schematic chart since the same steps are taken in both cases (in “B,” though, extra data sets are expected). The leftmost box of Figure 21 refers to the files obtained directly from the DMA, which can be given in text (*.txt) or Excel (*.xls or *.xlsx) formats. These files can either be obtained in

stress- or strain-controlled modes; thus the dashed box is identified by the general term "Oscillatory data." As can also be noticed, on the rightmost side of Figure 21 is a box named "Output files." According to what is indicated in the box, two files are generated by the software, one corresponding to the analysis of the specimens in dry condition and another to that of specimens in wet condition. It is important, however, to make it clear that the software does not need both dry and wet conditions to run. It is up to the user to decide if the analysis will be run on both conditions or only on one of them. Moreover, it is necessary to clarify that only one kind of mix can be analyzed at a time, meaning that data corresponding to different mixes should be loaded at different times.

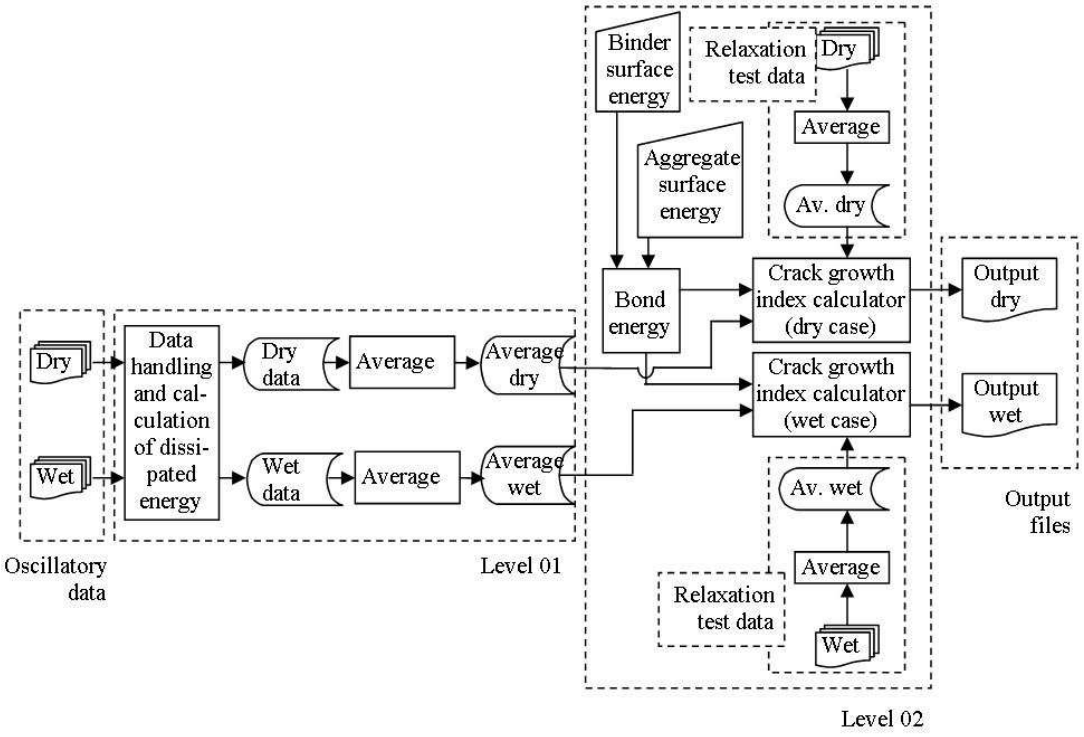

Figure 21: Software architecture and program flow.

Implementation

The execution steps of the software may be divided into five distinct operations: (i) acquire information about test setup, (ii) read data from oscillatory tests, (iii) acquire information on

surface energies of aggregates and binder used, (iv) read data from linear viscoelastic relaxation tests, and (v) perform calculations and write output files. Steps (i) and (ii) correspond to analysis Level 01, with step (ii) only being executable after step (i) is finalized. On the other hand, steps (iii) and (iv) correspond to Level 02, but, in this case, the steps can be executed independently. It is important to notice that step (v) is executed as the other steps are finalized and output data are generated.

This does not mean parallel processes are being executed, but rather that the output file is being generated as a consequence of data entered by the user at a given moment. The first version of the software does not support asynchronous processing and, because of that, the above-mentioned steps have to follow a fixed order. Hence, step (i) is followed by steps (ii), (iii), and (iv), in this order, whereas step (v) is executed as needed throughout this process by the use of the class DMA, indicated in Figure 22. Class DMA holds not only the user interface settings, but also internal functions that are capable of computing the desired values for analysis, as well as the guidelines to generate the output file in Microsoft Excel format. This class depends, however, on the information stored in the static class DataProcess.

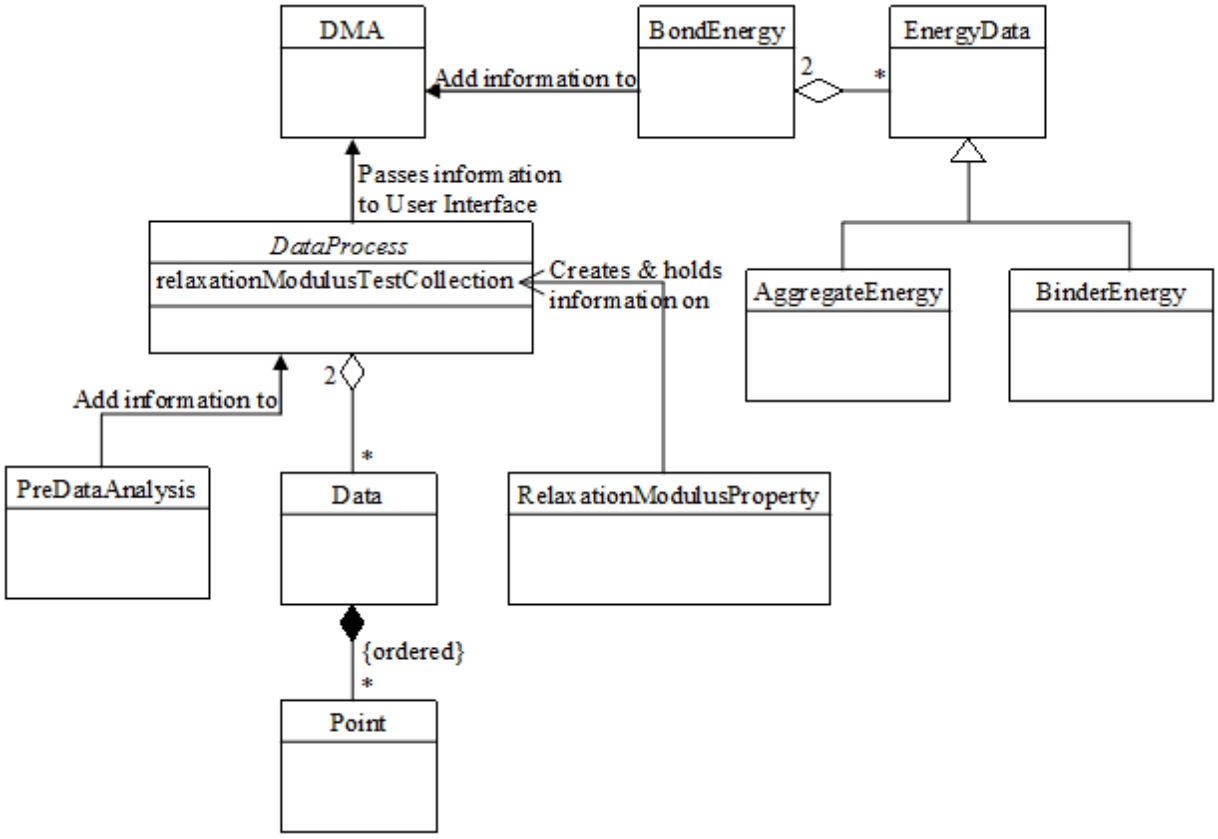

Figure 22: Framework of class organization in implementation.

Static classes are those where all members are static. The “static” keyword in C# refers to members that are invoked directly from the class level, i.e., those that do not need to use an instance (object) of that class (Troelsen 2007). When this keyword is applied to a whole class, all methods and fields (thus, all members) become static themselves. This kind of class is used to group data and functions that do not require to be instantiated (Solis 2008). As a natural consequence of this definition, static classes are also abstract, but with the difference that no other class can inherit from them. In this sense, DataProcess is the class that stores all data from the experimental tests given as input by the user – steps (ii) and (iv) – as well as any specific information about these tests – steps (i) and (iii). It also performs intermediate operations required by class DMA, such as interpolations, averages, and logarithmic calculations, thus the name of the class. The advantages of using a static class is that, first, no memory needs to be allocated to objects of that class; second, its methods and fields can be accessed at anytime

during the execution of the program; third, it is more type-safe (i.e., it avoids improper conversions between types more efficiently); and, finally, it presents a cleaner and more organized solution (Prata 2005, Troelsen 2007, Solis 2008).

DataProcess is formed by a set of different data from oscillatory tests performed in both dry and wet conditions. Each of these test conditions result in two lists inside DataProcess that store information on the dry and wet data. These lists are called dataCollectionDry and dataCollectionWet. The “data” part at the beginning of the variable names refers to the kind of class those lists store: class Data, as presented in Figure 22. One instance of Data is created for every loaded test. Each one of these objects stores data sets obtained directly from the test files, but it also invokes DataProcess methods so it can store specific information about every test. Figure 23 shows the fields where the information is stored. General information (i.e., those common to all tests) is stored in DataProcess itself through the use of the class PreDataAnalysis – invoked before any file has been read. The class Data is formed by a collection – or a composition, as indicated by the black diamond in Figure 22 (Fowler 2004) – of objects of type Point. Point is a simple type defined in order to store information for each experimental point acquired by the DMA machine when performing the oscillatory tests, as well as some of the intermediate results obtained after brief data handling done by DataProcess.

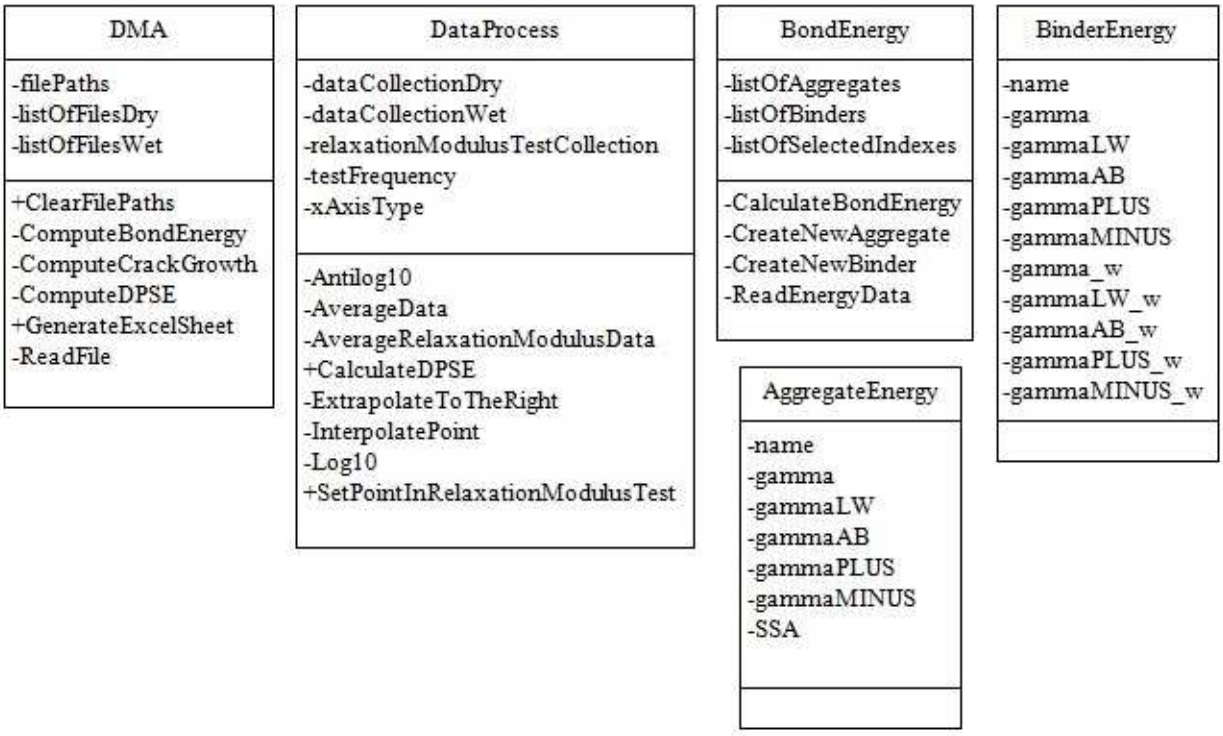

Figure 23: UML representation of main classes.

As can be seen in equation (14), the crack radius index depends on different variables. These variables are obtained by two separate sets of data: one from the bond energies between asphalt binder and the aggregate (in the presence of water or not) and the other one from the relaxation modulus tests. These correspond to the mentioned steps (iii) and (iv), respectively, and originate the classes BondEnergy (Figure 23) and RelaxationModulusProperty, in the same order.

Like the class DMA, BondEnergy is formed by data storage and internal processes, but it also serves as a graphical user interface (GUI). From this GUI the user can choose from two lists which binder and which aggregate(s) were used in his or her mix. These lists are loaded from data files given during the software installation process. These files can be manipulated directly from the original file or from the software, where users have the option to add new materials, according to their needs. For this reason, BondEnergy is represented by two aggregations of class EnergyData, which is an abstract class that will originate two child classes: AggregateEnergy and BinderEnergy. One of the aggregations inside BondEnergy is

called listOfAggregates and the other one listOfBinders. After the proper binder has been selected, in association with as many aggregates as the user wants, the information is given to DMA class, which can process and perform the pertinent computations.

The class RelaxationModulusProperty is responsible for reading the files from relaxation modulus tests provided by the user. After reading all points, these data are stored in DataProcess in the form of a list in which each element is in fact another list of ordered pairs. These pairs correspond to the value of the relaxation modulus at a given time. The main list variable is called relaxationModulusTestCollection. All operations, including the regression to the curve given by equation (15), is done by DataProcess. The most important information extracted from step (iv), however, is the average result of the experimental data, which will serve as base for the variables needed in equation (14).

Software validation

The results generated with the software were compared to the output obtained from a MATLAB routine, in use for more than 2 years at the Texas Transportation Institute (TTI). This code implements an analysis that corresponds to Level 01A. The validation was made by comparison of results given by both programs when the same file is loaded.

The results found were, in most cases, exactly the same for MATLAB and the software. Four parameters of comparison were studied, out of which three coincided in both analyses. These three parameters were: the curve $\left(N\left|G^*_{N,F}\right|\right)/G_R$ vs. N, fatigue life (the maximum of that curve), and curve $W_R(N)$ vs. N. The only parameter that differed between the analyses was the value of b (from equation (13)). This, however, was predictable because of two factors. First, this parameter depends on the regression of scattered data to a given curve, which may be done by different methods. Since the method adopted by MATLAB differs from that used in Microsoft Excel, distinct solutions are found. Second, the domain onto which the regression is applied is also different in each case. This results in a ratio (software/MATLAB) of approximately *1.1* and *0.85* between the b values generated by each method for the dry and wet Texas mix, respectively (Table 9).

Table 9: Differences between parameters found with the use of MATLAB and the developed software.

Method	Dry		Wet	
	b value	Coefficient of variability	b value	Coefficient of variability
MATLAB	1773.78	14.9%	1817.92	19.7%
Software	1576.25	14.2%	2130.01	32.3%

This difference in the b value has little effect in the crack radius index calculation if one considers the inherent variability of fatigue-life tests. At 30,000 cycles, the ratio between the crack radius indexes, as calculated by the software and by MATLAB, is 0.994 for the dry mix. In the case of the wet mix, the ratio of the crack radius indexes between the software the MATLAB (with manual calculations) is 0.803.

The quality of the fit given by the software and MATLAB is equivalent in terms of the b value. Despite the difference of up to 30% in the slope values found by both methods, they result in visually good fits. No error parameter was used to analyze and compare the results because the MATLAB regression generates improper a values to equation (13). Figure 24 presents an example of plots of the experimental data and the original fits from MATLAB and the software, besides the MATLAB line vertically shifted by an arbitrary coefficient.

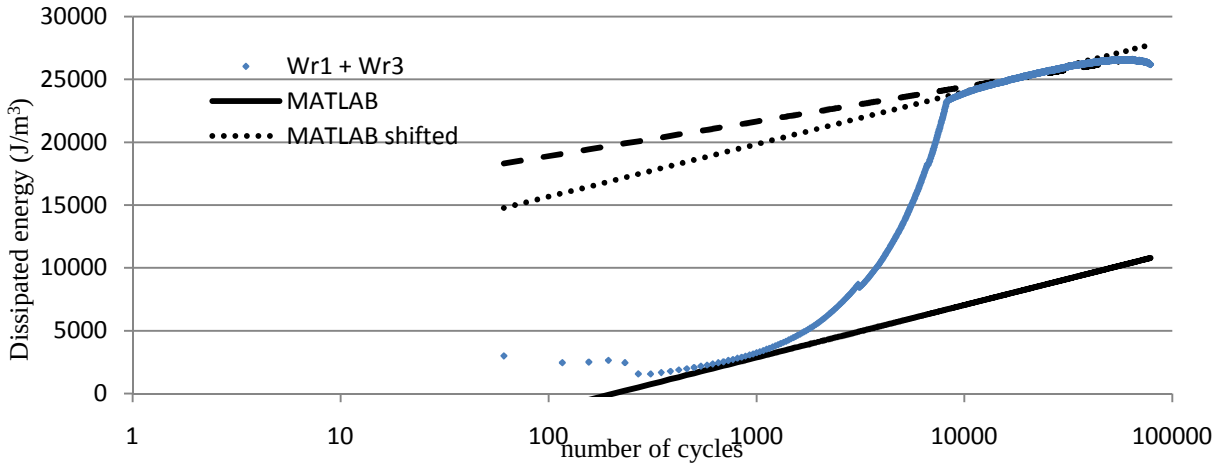

Figure 24: Comparison between linear regressions from MATLAB and the software.

CHAPTER V
CONCLUSIONS AND RECOMMENDATIONS

The benefits of introducing a comprehensive test methodology to FAM mixtures are reflected by the fact that (i) the new design protocol is simple and does not demand any special apparatus, being applicable in any asphalt laboratory; (ii) despite the empiricism of the method, the procedure is highly repeatable, generating consistent values for different specimens with a low standard deviation; (iii) the asphalt binder content in the FAM mix is related to the original full asphalt mix by properties directly measured from the mix; (iv) all specimens can be mixed, compacted, and cored with no problems; and (v) dry condition has a similar performance to that seen on the old method concerning crack formation and crack propagation, whereas moisture susceptibility is accentuated, allowing for a better judgment on mixes performance under wet conditions.

On the other hand, the method is purely empirical and thus may not account for all the factors expected to play important roles in the FAM, such as the real air voids structure or the moisture diffusion inside the full mix. The specimens obtained from this method are, in general, too rigid, which may be a problem depending on the torque limits of the DMA equipment in use. Another problem that may be faced when using the method is that the low asphalt content may make mixing difficult. It is recommended that a thorough mix be accomplished before compaction; otherwise samples might get become porous and/or present uncoated aggregates.

The object-oriented paradigm, in association with the use of Graphical User Interfaces, has shown not only to be useful to the development of future research in this field, but also has provided a functional tool for pavement designers. This new tool allows the analysis of data from DMA tests without any required knowledge on the theory is of great contribution to the field of study. This will result in the creation of a new database, which will lead to the creation of important parameters in pavement design. The software developed allows for two levels of analysis, depending on the kind of data available. The results obtained from the software have shown to be precisely the same as those obtained by manual manipulation of the data and close to those obtained in other publications. Considering the inherent variance of stress- and strain-

controlled tests and the fact that new oscillatory tests were performed, having been able to qualitative reproduce results shown in other publications is a proof of good performance.

The analysis methodology embedded in the software is based on energy criteria. At a simpler level, the dissipated energies between different asphalt mixes are compared to each other. A higher energy level means that, for a given number of cycles, more energy was dissipated out of the system, that is, more damage was induced. The ratio of energy between mixes allows for performance comparisons, whereas the ratio between dry and wet conditions of a same mix renders information on the moisture susceptibility. The values of dissipated energy are given at two distinct moments: at 5,000 and 50,000 cycles. Even if the analysis at 50,000 cycles generally generates more consistent results, not all tests reach this far, thus the necessity of including the results at a lower number of cycles. The second level takes into consideration the adhesion energy that bonds asphalt binder and the aggregate surface together. It also accounts for the presence of water in this interface and thus is more capable, as a model, of producing better results. Moreover, the model allows for the prediction of crack formation inside the mix, as well as for crack propagation, being very useful on the study of the lifespan of asphalt mixes.

Concerning the future research to be developed from the achievements of this work, one should consider improving the new method of design: the empirical results obtained from the execution of the method may be linked to physical and chemical characteristics of the mix, binder, and aggregates. It is thus recommended the use of Aggregate Imaging System and surface bond energy to try to back-calculate the design binder content of different mixes.

The software was built having in mind future expansions. It can easily accommodate new modules that will allow running probabilistic analyses, such as that presented in Caro (2008). Another possible improvement is giving the software the capability of loading multiple mixes at the same time and generating on single output file where all data would be summarized. It may also be re-engineered to be executable in other working platforms other than those based on Microsoft Windows.

REFERENCES

American Association of State Highway and Transportation Officials, 2006. *AASHTO T 327: Standard method of test for resistance of coarse aggregate to degradation by abrasion in the Micro-Deval apparatus.* Washington, DC.

American Association of State Highway and Transportation Officials, 2008a. *AASHTO T 85: Specific gravity and absorption of coarse aggregate.* Washington, DC.

American Association of State Highway and Transportation Officials, 2008b. *AASHTO T 209: Theoretical maximum specific gravity and density of bituminous paving mixtures.* Washington, DC.

American Association of State Highway and Transportation Officials, 2009. *AASHTO T 308: Standard method of test for determining the asphalt binder content of hot mix asphalt (HMA) by the ignition method.* Washington, DC.

Bhasin, A., Masad, E., Little, D. and Lytton, R., 2006. Limits on adhesive bond energy for improved resistance of hot mix asphalt to moisture damage. *Transportation Research Record: Journal of the Transportation Research Board.* Washington, DC, 1970, 3–13.

Caro, S., Masad, E., Airey, G., Bhasin, A. and Little, D.N., 2008. Probabilistic analysis of fracture in asphalt mixes caused by moisture damage. *Transportation Research Record: Journal of the Transportation Research Board*. Washington, DC, 2057, 28–36.

Castelo Branco, V.T.F., 2008. *An unified method for the analysis of nonlinear viscoelasticity and fatigue cracking of asphalt mixes using the dynamic mechanical analyzer*. Ph.D. dissertation . Texas A&M University, College Station.

Christensen, R.M., 1982. *Theory of viscoelasticity*. New York: Academic Press.

Findley, W.N., Lai, J.S. and Onaran, K., 1989. *Creep and relaxation of nonlinear viscoelastic materials*. New York: Dover Publications, Inc.

Fowler, M., 2004. *UML distilled: A brief guide to the standard object modeling language*. 3rd ed. Boston, MA: Pearson Education, Inc.

Gdoutos, E.E., 2005. *Fracture mechanics: an introduction*. 2nd ed. Dordrecht, Norwell, MA: Springer.

Huang, Y.H., 2004. *Pavement analysis and design*. 2nd ed. Upper Saddle River, NJ: Pearson Prentice Hall.

Kim, Y.R. and Little, D.N., 2003. *Development of specification-type tests to assess damage and healing properties of bitumens and mastics.* FHWA/473630. Federal Highway Administration, Texas Transportation Institute, Texas A&M University, College Station.

Kim, Y.-R. and Little, D.N., 2004. Linear viscoelastic analysis of asphalt mastics. *Journal of materials in civil engineering*, 16, 122–132.

Kim, Y.R., Little, D.N. and Song, I., 2003. Effect of mineral fillers on fatigue resistance and fundamental material characteristics: mechanistic evaluation. *Transportation Research Record: Journal of the Transportation Research Board.* Washington, DC, 1832, 1–8.

Leventhal, L. and Barnes, J., 2008. *Usability engineering: Process, products, and examples*. Upper Saddle River, NJ: Prentice Hall.

Lytton, R.L., Uzan, J., Fernando, E.G., Roque, R., Hiltmen, D. and Stoffels, S., 1993. *Development and validation of performance prediction models and specifications for asphalt binders and paving mixes.* Strategic Highway Research Program Report A-357. Washington, DC: SHRP, National Research Council.

Mandel, T., 1997. *The elements of user interface design*. New York: John Wiley & Sons, Inc.

Masad, E., Castelo Branco, V.T.F., Little, D.N. and Lytton, R.L., 2006a. *Analysis of mastic damage using stress controlled and strain controlled test.* FHWA-473630. Federal Highway Administration, U.S. Department of Transportation, Washington, DC.

Masad, E., Castelo Branco, V.T.F., Little, D.N. and Lytton, R., 2008. A unified method for the analysis of controlled-strain and controlled-stress fatigue testing. *International Journal of Pavement Engineering*, 9 (4), 233–246.

Masad, E., Zollinger, C., Bulut, R., Little, D. and Lytton, R., 2006b. Characterization of HMA moisture damage using surface energy and fracture properties. *Journal of the Association of Asphalt Paving Technologists*, 76, 713–754.

McLaughlin, B.D., Pollice, G. and West, D., 2007. *Head first object-oriented analysis and design*. Sebastopol, CA: O'Reilly Media, Inc.

Mindess, S., Young, J.F. and Darwin, D., 2003. *Concrete*. 2nd ed.. Upper Saddle River, NJ: Prentice Hall.

Papagiannakis, A.T. and Masad, E.A., 2008. *Pavement design and materials*. Hoboken, NJ: John Wiley & Sons, Inc.

Prata, S., 2005. *C++ primer plus*. 5th ed. Indianapolis: Sams Publishing.

Roberts, F.L., Kandhal, P.S., Brown, E.R., Lee, D.Y. and Kennedy, T.W., 1996. *Hot mix asphalt materials, mix design, and construction*. Lanham, MD: NAPA Education Foundation.

Schapery, R.A., 1973. *A theory of crack growth in viscoelastic media.* Office of Naval Research, Department of the Navy. Task Order NR 064-520. Technical Report No. 2. Texas A&M University, College Station.

Solis, D., 2008. *Illustrated C# 2008*. 1st ed. New York: Apress.

Stone, D., Jarrett, C., Woodroffe, M. and Minocha, S., 2005. *User interface design and evaluation*. San Francisco: Morgan Kaufman.

Stroustrup, B., 1997. *The C++ programming language*. 3rd ed. Reading, MA: Addison-Wesley.

Troelsen, A., 2007. *Pro C# 2008 and the .NET 3.5 platform: using the .NET universe using curly brackets*. 4th ed. New York: Apress.

Vasconcelos, K., Bhasin, A., Little, D. and Soares, J., 2007. *Evaluation of moisture damage and healing in mastic.* 18th Asphalt Meeting, IBP, Rio de Janeiro, Brazil (in Portuguese).

Yoder, E.J. and Witczak, M.W., 1975. *Principles of pavement design*. 2nd ed. New York: John Wiley and Sons.

Zollinger, C., 2005. *Application of surface energy measurements to evaluate moisture susceptibility of asphalt and aggregates*. Thesis, (M.S.), Texas A&M University. College Station.

APPENDIX A

STANDARD METHOD FOR PREPARING DYNAMIC MECHANICAL ANALYZER (DMA) SPECIMENS

DISCLAIMER

This work was performed by a task force group at Texas Transportation Institute, Texas A&M University. The professionals in charge of this standard method are Pedro Sousa and Veronica T.F. Castelo Branco.

1. SCOPE

This document presents the procedures for specimen preparation and mixture design of fine aggregate matrix (FAM) to be tested in the dynamic mechanical analyzer (DMA).

2. REFERENCED DOCUMENTS

AASHTO Standards:

- T 312-04, Preparing and Determining the Density of the Hot Mix Asphalt (HMA) Specimens by Means of the Superpave Gyratory Compactor
- T 166, Bulk Specific Gravity of Compacted Hot Mix Asphalt Using Saturated Surface-Dry Specimens
- T 209, Theoretical Maximum Specific Gravity and Density of Bituminous Paving Mixtures
- T 308, Standard Method of Test for Determining the Asphalt Binder Content of Hot Mix Asphalt (HMA) by the Ignition Method.
- T 327, Standard Method of Test for Resistance of Coarse Aggregate to Degradation by Abrasion in the Micro-Deval Apparatus
- T 316, Viscosity Determination of Asphalt Binder Using Rotational Viscometer

3. SIGNIFICANCE AND USE

This standard defines the preparation of Fine Aggregate Matrix (FAM) mixes. The design method of FAM links it to the original binder content of the full asphalt mix by empirical lab procedure.

Annexes A and B follow the AASHTO style for standard formats.

4. SUMMARY OF TEST METHODS

The design methodology of DMA mixtures attempts to obtain a FAM that is representative of a full asphalt mixture (i.e., HMA). For this reason, a previously established HMA design is required for this process. The design procedure of FAMs only utilizes the granular material of the HMA mixture that passes the sieve #16 (1.18 mm opening). The asphalt content of the FAM is obtained by sieving the HMA through a sieve #16 and submitting the passing material to an ignition oven test.

The first step in the preparation of the specimens consists of mixing and compacting, using the Superpave gyratory compactor (SGC), to obtain a 150 mm diameter cylindrical sample with an approximate height of 90 mm. This procedure is similar to the one used to prepare regular HMA specimens. The upper and lower parts of the cylinders are sawed in order to produce a new cylinder 150 mm in diameter and 50 mm high. This compacted sample is cored into small DMA cylindrical specimens 12 mm in diameter and 50 mm high. Each specimen is properly labeled and prepared for testing

5. APPARATUS

5.1. Calipers—digital or analog calipers with an accuracy of ±0.005 in. (0.01 mm).

5.2. Balance—the standard balance meeting.

5.3. Small pans—used to take the sieved HMA to the ignition oven should be small enough not to exceed the limit of the balance, but also large enough to fit the whole sample. Pans like the ones used for the Pressure Aging Vessel test are indicated as a good size.

5.4. Ignition oven—the furnace and its accessories as described in AASHTO T 308.

5.5. Other apparatus—other apparatus required to perform the procedures described in this document include an oven and a SGC.

6. HAZARDS

Observe standard safety precautions when preparing HMA specimens.

7. MIXTURE DESIGN

FAM samples are composed by fine aggregates (smaller than 1.18 mm, including filler) and asphalt binder. The materials (fine aggregates and binder) are related to the reference HMA mixture. Two procedures to estimate the binder film thickness in those mixtures are presented.

7.1. Obtain the following information for the HMA: (i) aggregate gradations and (ii) percentage of binder. The series of sieves used should include No. 16 (1.18 mm) and No. 30 (0.60 mm) sieves.

7.2. Identify the HMA aggregates that pass the No. 16 (1.18 mm) sieve. Develop the FAM gradation curve, keeping the same proportions for each aggregate passing the No. 16 (1.18 mm) sieve (see Figure A.1).

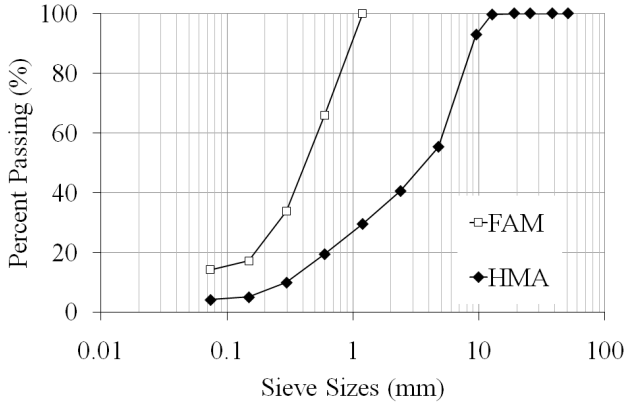

FIGURE A.1—Hot Mix Asphalt and Fine Aggregate Matrix Gradation Curves

7.3. Establish the aggregates batch size (in grams) that will be used to compact the FAM sample according to the mold diameter and the desired sample height.

7.4. Calculate the weights of each size fraction of the aggregate required for one batch of the FAM. Use the gradation developed in step 7.3.

7.5. Prepare three samples of the HMA for which the FAM needs to be determined. The minimum mass for each sample is given by Table A.1.

TABLE A.1—Minimum sample sizes.

Nominal Maximum Aggregate Size (mm)	Minimum Sample Size (g)
Greater or equal to 37.5	4,000
19 or 25	2,500
Lesser or equal to 12.5	1,500

7.6. Separate the HMA particles by hand. This will prevent possible fracturing of the aggregates. If the HMA is not soft enough to be partitioned by hand, it should be warmed up in a flat pan until so.

7.7. Transfer the asphalt mix to an oven at 135°C where it will be conditioned for a two hours period which will ensure the computation of realistic values for the amount of asphalt absorbed by the aggregate and void properties of the mix, as described in AASHTO T 209.

7.8. Sieve the HMA through a sieve No16 with the help of a mechanical sieving machine. The use of 9.5mm stainless steel balls (from the micro-deval apparatus – AASHTO T 327) is recommended to help separating the particles that stick together.

7.9. Oven dry the material that passes sieve No16 to a constant mass at a temperature of 110°C.

7.10. Separate and weigh pans on a balance with a minimal precision of 0.001g. The weight obtained for each pan should be wrote down as W_P. Transfer the material that is in the oven to the pan and weigh it again. The value obtained is written as W_M. The pans with the materials should not exceed the limit of the balance and should also allow the material to be spread on a thin layer.

7.11. Put the pan in an ignition oven apparatus (AASHTO T 308) for the asphalt binder present in the sieved material to be burned. Burning is considered complete after three minutes with no change in mass superior to 0.01%. A minimum burning time of 10 minutes is also required.

7.12. Remove the pan from the furnace and place over a cooling plate or block, where it should rest for approximately 30 minutes, properly covered with a protective cage.

7.13. Weigh the pan and burnt material and write down the obtained value as W_A.The percent of binder is calculated by the formulation below.

$$P_b = \frac{W_M - W_A}{W_M - W_P} \times 100\% \quad (2)$$

10 MIXTURE PREPARATION

The preparation of cylindrical specimens for use in DMA tests (i.e., DMA specimens) consists of four parts.

8.1. Prepare a 150-mm (6-in.) compacted sample of the fine-aggregate–portion asphalt mixture in the SGC. In this step, the job formula for the HMA mixture, the binder properties (for determining the amount of binder, and the mixing and compacting temperatures), and the value of the theoretical maximum specific gravity of the FAM are required. The mixing and compacting temperatures should be calculated from the results of viscosity according to the AASHTO T 316 procedure.

8.1.1. Conduct a mixture preparation and compaction of a 150 mm (6 in.) specimen in the SGC, following most of the steps specified in AASHTO T 312-04. A summary of the procedure follows:

- According to the DMA mixture design process (Section 7), weigh each aggregate fraction that makes up the mixture and combine them in a pan.
- Mix the portions and place the fine aggregate material in a pan, taking special care not to lose the finest portion (material passing the No. 200 sieve) during the process.
- Leave the pan in the oven overnight at the mixing temperature.
- Place the binder and all the elements required for mixing (spoons, can, etc.) in the oven at the mixing temperature for 2 h (or the time required for the binder to become a liquid) before the mixing process.
- Take the fine aggregate material and the mixing can out of the oven and weigh the total amount of material that was calculated for the batch. Take the binder out of the oven and pour the corresponding amount of asphalt binder into the can, according to the mixture formula.
- Move the material to the mixing can, taking special care not to lose the finest portion of the material.
- Mix the material until all of the granular material seems to be homogeneously coated by the binder (at least 2 min in the mechanical mixer).
- Perform a 2 h short-term aging process by placing the loose mixture in the oven at the mixing temperature.
- Place all the elements that are going to be required during the compaction process (mold, spoons, etc.) in the oven at least 30 min prior to compaction.
- After 2 h, remove the material from the oven and follow the compaction process according to AASHTO T 312-04. The following specifications should be used as inputs in the gyratory compactor:
  - Angle: 1.25±0.02°
  - Pressure: 600±18 kPa
  - Criteria of termination: use the percent of voids specified in the design, the mass of the batch, and the maximum specific gravity of the mixture to determine a termination criterion for compaction (height or density). Compaction until constant height (maximum compaction) is also acceptable.
- Allow the sample to cool and then remove the sample from the mold. The wait time depends on the amount of binder used. It might vary from 2 to 90 minutes.
- Label the sample.

Figure A.2 presents a final sample obtained from this process.

FIGURE A.2—150 mm (6 in.) Diameter Sample

8.1.2. Allow the sample to cool for at least 3 h.

8.1.3. Calculate the air voids content of the FAM. It is possible to use the AASHTO T 166 procedure or the Corelock® procedure (using program number 1). Verify that the air void content is in the expected range according to the mixture design formula. If there is a difference of more than 15 percent between the expected and the actual air void content, verify the compaction process (especially the termination criterion) and repeat the previous process. If the air void content is acceptable, continue with the next step.

8.2. Core the compacted sample.

8.2.1. Saw the upper and lower parts of the cylindrical sample to obtain a new cylinder with the same diameter (150 mm) but with a 50 mm height (see Figure A.3).

(a) (b)

FIGURE A.3—Sawing Process (a) and Final Result (b)

8.2.2. Allow the core to dry completely for at least 4 h (using a fan during the process is recommended).

8.2.3. Calculate the air voids content of the core following the same procedure used in Section 8.1.3.

8.2.4. Core the DMA cylindrical specimens that are 50 mm high and 12 mm in diameter. The velocity used during the coring process is a relevant parameter in determining the quality of the sample. To avoid damaging the top of the DMA sample, it is recommended that the SGC sample be placed between the parts cut from the top and bottom of the cylinder during the coring procedure.

8.2.5. Immediately after each specimen is obtained, label it as A, B, or C, where A corresponds to the inner concentric zone of the core, B to the intermediate zone, and C to the outer zone (see Figure A.4). Also include a number for each sample in each zone (i.e., C4 is the fourth sample that was obtained for the outer zone). Each sample should also contain a mark indicating the border that corresponds to the upper part of the original

compacted specimen. Obtaining at least 24 DMA samples in total from a 150 by 50 mm core is recommended. A typical value of total DMA specimens is 30 samples; a maximum value is approximately 32 samples.

FIGURE A.4—Coring DMA Specimens

8.2.6 Allow the samples to dry completely for at least 4 h (a fan is recommended).

8.2.7 Calculate the air voids content of at least five samples in each group (i.e., A, B, and C). To do so, follow a procedure similar to the one indicated in AASHTO T 166, but adapt a small balance in order to measure the weight of the saturated sample underwater. If the air voids in specimens belonging to the same group differ by more than 35 percent, select three new specimens and repeat the measurements. If the differences continue, review the other groups. If all groups present this difference or the differences among the average air void content of the three groups is higher than 35 percent, or both, repeat the experiment.

8.2.8 Select at least eight specimens corresponding to the zone having the average air void content closest to the design value. Take into account the variability of the results obtained in Section 8.2.7 and the number of samples available in each group.

9. KEYWORDS

Fine Aggregate Matrix (FAM).

ANNEXES

A1. FINE AGGREGATE MATRIX DESIGN EXAMPLE

A1.1. Consider an HMA mixture that contains: 22 percent #8 limestone, 22 percent #8 gravel, 10 percent limestone sand, 26 percent natural sand, and 20 percent recycled asphalt pavement (RAP). The binder percentage used was 5.4 percent by weight of the total mixture. The aggregates gradation and mixture blend are in Table A.2.

TABLE A.2—Hot Mix Asphalt Aggregates Gradation and Mixture Blend

Sieve Size (mm)	Aggregate (% Passing)					Blend (% Passing)
	#8 Limestone	#8 Gravel	Limestone Sand	Natural Sand	RAP	
50.80 (2 in.)	100	100	100	100	100	100
37.50 (1-1/2 in.)	100	100	100	100	100	100
25.40 (1 in.)	100	100	100	100	100	100
19.05 (3/4 in.)	100	100	100	100	100	100
12.70 (1/2 in.)	100	100	100	100	98	100
9.50 (3/8 in.)	88	95	100	100	83	93
4.75 (#4)	18	20	100	100	55	55
2.36 (#8)	2	2	90	92	34	41
1.18 (#16)	2	2	63	67	25	30
0.60 (#30)	2	2	40	44	16	20
0.30 (#50)	2	2	20	18	12	10
0.15 (#100)	2	2	9	5	10	5
0.075 (#200)	2	2	6.4	4.3	7.6	4

A2.2. For the DMA mixture, only aggregates smaller than 1.18 mm (passing the No. 16 sieve) are used, so aggregate quantities should be proportionate again. The DMA mixture contains, for this example: 1.5 percent #8 limestone, 1.5 percent #8 gravel, 21.3 percent limestone sand, 58.9 percent natural sand, and 16.8 percent RAP. These values were found by multiplying the HMA aggregate contribution by the amount of each aggregate passing the No. 16 sieve and then dividing this product by the percent of the blend that passes the No. 16 sieve. For example, the amount of #8 limestone that should be used in the DMA mixture was found:

$$Ammount\ of\#8\ limestone\ DMA = \frac{0.22 \times 0.02}{0.30} = 1.5\% \quad (12)$$

A2.3. The aggregates gradation and mixture blend for the DMA are in Table A.3. Note that aggregates gradations were also proportionate again.

TABLE A.3—Fine Aggregate Matrix Gradation and Mixture Blend

Sieve Size (mm)	Aggregate (% Passing)					Blend (% Passing)
	#8 Limestone	#8 Gravel	Limestone Sand	Natural Sand	RAP	
1.18 (#16)	100	100	100	100	100	100
0.60 (#30)	100	100	63.5	65.7	64	66
0.30 (#50)	100	100	31.8	26.9	48	34
0.15 (#100)	100	100	14.3	7.5	40	17
0.075 (#200)	100	100	10.2	6.4	30.4	14

A2.4. In order to calculate the amount of binder by weight that should be used in the DMA mixture, HMA gradation should be considered. Assume a mixture batch size of 4,500 Kg. Calculate the mass of the aggregate blend retained by each sieve (see Table A.4).

TABLE A.4—Mass of Aggregate Blend Retained by Each Sieve

Sieve Size (mm)	% Retained	Mass (g)
50.80 (2 in.)	0.0	0.00
37.50 (1-1/2 in.)	0.0	0.00
25.40 (1 in.)	0.0	0.00
19.05 (3/4 in.)	0.0	0.00
12.70 (1/2 in.)	0.4	17.0
9.50 (3/8 in.)	6.7	286.9
4.75 (#4)	37.5	1,596.4
2.36 (#8)	14.8	628.3
1.18 (#16)	11.0	468.3
0.60 (#30)	10.1	429.1
0.30 (#50)	9.6	407.0
0.15 (#100)	4.9	207.7
0.075 (#200)	0.9	39.3
Pan (passing on #200 sieve)	4.2	177.0

A2.5. Add the mass of any aggregate smaller than 1.18 mm. The mass of aggregates smaller than 1.18 mm for this example is 1,260.07 g.

APPENDIX B

STANDARD METHOD FOR CONDUCTING DYNAMIC MECHANICAL ANALYZER (DMA) TESTS

DISCLAIMER

This work was performed by a task force group at Texas Transportation Institute, Texas A&M University. The professionals in charge of this standard method are Jonathan Howson, Kamilla L. Vasconcelos, Silvia Caro, Veronica T.F. Castelo Branco and Pedro Sousa.

1. SCOPE

This document presents the procedures for testing and data analysis of fine aggregate matrix (FAM) to be tested in the dynamic mechanical analyzer (DMA). The document also explains how the results obtained by these procedures can be used in a more complex fracture mechanics model that characterizes bituminous materials.

2. REFERENCED DOCUMENTS

AASHTO Standards:

- T 209, Theoretical Maximum Specific Gravity and Density of Bituminous Paving Mixtures

3. SIGNIFICANCE AND USE

This standard is used to characterize the rheological properties of FAM. The standard refers to two different tests that can be performed using the DMA apparatus: (i) shear oscillation (time sweep) and (ii) relaxation modulus. These tests provide relevant information regarding the behavior of the HMA fine matrix, which is composed of fine aggregates (particles passing the No. 16 [1.18 mm] sieve) and asphalt binder.

The results from these procedures can be used to

- determine the fatigue life at different test conditions (i.e., temperature or frequency, or both);
- characterize the continuous damage of the sample in terms of the dissipated pseudo-strain energy as a function of the number of cycles;
- determine the relaxation modulus as a function of time, i.e., $E(t)$,
- use the data obtained from oscillation and relaxation tests in a model based on viscoelastic fracture mechanics principles to characterize fatigue damage phenomena; and

- evaluate moisture-damage susceptibility using the same fracture mechanics model (this analysis provides important information about the moisture susceptibility of the FAM tested).

4. SUMMARY OF TEST METHODS

The DMA test provides fundamental information regarding the rheological properties of the fine matrix portion of asphalt mixtures.

Each specimen must be labeled and prepared before testing. Two methods of test-specimen preparation are considered herein: (i) testing under dry condition and (ii) testing specimens that have been subjected to a moisture conditioning process.

Two tests that are performed using the DMA apparatus are described in this document:

- Shear oscillation (time sweep) test
- Relaxation modulus test

The oscillation test is conducted on an average of six DMA specimens (depending on the coefficient of variation). The test is conducted in controlled-strain or controlled-stress modes using the oscillation procedure, and has two main parts: (i) 2 min of oscillation at low constant strain/stress amplitude and (ii) a fatigue test at a higher constant strain/stress amplitude. Both tests are performed at a fixed frequency. The low and high strain/stress amplitudes should be determined from the results of a strain/stress sweep test according to the following criteria: the low strain/stress should guarantee that the material's behavior is in the linear viscoelastic region (a value of 0.001 percent strain or 3.20×10^3 Pa is commonly used for controlled-strain and controlled-stress tests, respectively). The high strain/stress amplitude should produce an initial damage behavior of the material (a value in the range of 0.1–0.4 percent or 9.0×10^4–2.00×10^5 Pa is commonly used for controlled-strain and controlled-stress tests, respectively). Ideally, the high strain/stress amplitude should be on the threshold between the nonlinear viscoelastic region and the damage region. Other practical considerations in the selection of these values (e.g., total time of testing, time before failure, etc.) should also be taken into account. The oscillation test is normally conducted at room temperature, although the effect of temperature can be analyzed by repeating the procedures described above at different temperatures. Depending on the DMA equipment used, the torque necessary to reach the strain/stress level may exceed the machine limit. In this case, tests should be run at a higher temperature (30°C has been shown as a reasonable choice). To assess the moisture-damage susceptibility of the material, it is necessary to use DMA specimens that have been subjected to a moisture conditioning process (see Section 7).

The relaxation properties of the FAM can be obtained from a relaxation test. The test should be performed on at least three DMA specimens using a step-load function at a constant shear-strain amplitude. The percent of shear strain should be the same strain selected in the first part of the oscillation procedure (i.e., low percent of strain). The raise strain time and the total time of the step load function should be determined according to the apparatus requirements and mixture characteristics. Typical values of 0.2–1 sec for the raise strain time and 3–6 min for the step load function are recommended. To assess the moisture-damage susceptibility of the material, it is necessary to repeat the previous procedure but use DMA specimens that have been subjected to moisture conditioning (see Section 8).

Several analyses regarding the characterization of FAM can be performed based on the data obtained from these tests, as follows: (i) linear and nonlinear viscoelastic properties, (ii) fatigue life, (iii) crack growth potential, and (iv) moisture susceptibility (see Section 9).

5. APPARATUS

5.1. DMA—the machine must meet or surpass the following requirements:

- Torque range: 0.1×10^{-6}–200×10^{-3} N.m
- Torque resolution: minimum 10^{-9} N.m
- Range for measurable speed: 10^{-8}–600 rad/s
- Range for detectable speed: 10^{-8}–600 rad/s
- Angular position resolution: minimum 0.05×10^{-6} rad
- Frequency range: 10^{-6}–150 Hz
- Gap resolution: minimum 1 micron
- Range for sample height: 1–50 mm
- Normal force measurement range: 0.1–2,000 g
- Environmental chamber temperature range: –20–150°C
- Environmental chamber temperature accuracy: ±1°C

In addition to the above requirements, the DMA must have attachments capable of handling 12 mm cylindrical samples. The software must provide the user with the following information based on the data acquired during the test:

- Maximum and minimum strain per cycle
- Maximum and minimum stress per cycle
- Phase angle per cycle
- Maximum and minimum torque per cycle
- Maximum and minimum displacement per cycle
- Preferably a minimum of 128 data points per cycle for the torque, stress, and strain with respect to time
- Time
- Temperature
- Frequency
- Normal force

Figure B.1 presents two commercial rheometers that satisfy the previous requirements.

(a) AR 2000 TA®

(b) CVOR-200 Bohlin®

FIGURE B.1—Dynamic Mechanical Analyzers

5.2. Pressurized air supply—a compressed air supply that is capable of supplying clean, dry, oil-free air at an approximate pressure of 30 psi (approximately 2 bars) at a flow rate of 50 L. The dew point of the air supply should be –20°C or better.

5.3. Calipers—digital or analog calipers with an accuracy of ±0.005 in. (0.01 mm).

5.4. Glue—must be able to withstand force applied to the sample by a machine and must bond well to the cylindrical sample and end caps.

5.5. End caps or holders—stainless steel pieces used to secure the sample in the DMA attachments for testing. They must be slightly larger than 12 mm in diameter and 2 mm deep.

5.6. Other apparatus—other apparatus required to perform the procedures described in this document include a recipient for the applied vacuum saturation.

6. HAZARDS

Observe standard safety precautions when testing HMA specimens.

7 SPECIMEN PREPARATION

7.1. Method I: Testing dry specimens

7.1.1. Take four specimens and use epoxy to glue the holders onto the specimens (see Figure B.2).

FIGURE B.2—Holders, Glue, and Specimens in the Gluing Process

7.1.2. Wait at least 1 h (or the time specified in the glue's directions) before installing the sample in the DMA.

7.1.3. Test the sample.

7.2. Method II: Testing moisture-conditioned specimens

7.2.1. Take the other four specimens and apply a thin layer of epoxy to the ends. The goal of this step is to facilitate the gluing process after the mixtures have been subjected to the conditioning process.

7.2.2. For moisture conditioning the sample, it is required to count with a container that allows applying vacuum into a material submerged in water. Metallic containers such as those specified in the procedures for determining the theoretical maximum specific gravity and density of bituminous paving mixtures (AASHTO T 209) can be utilized for this purpose.

- Weigh the sample in a dry condition, before starting the conditioning procedure.
- Place a porous stone at the bottom of the recipient.
- Fill half of the recipient with water.
- Put the sample on the porous stone. A maximum of three samples can be conditioned at the same time.
- Close the recipient and apply vacuum saturation at a pressure of 27 mmHg for 1 h.
- Remove the sample, dry the surface, and weigh the specimen.
- Using the information collected, calculate the level of saturation of the sample.

A minimum of 85 percent saturation level should be achieved with this process. If this is not the case (e.g., in samples with a low air void content), modify the time of vacuum saturation until the minimum required is achieved. If several mixtures are being tested for comparison purposes, use a unique time for vacuum saturation; otherwise, the differences in the damage generated in the sample will produce a false comparison analysis.

7.2.3. After conditioning, wait 30 min before gluing the holders to the specimens. Follow the same procedure specified for Method I.

7.2.4. After waiting 2 h after gluing, perform the test as specified for Method I.

Note: A specimen that has been conditioned should be tested in the following two days, or it should be discarded.

7.3. Examine storage considerations

The total testing procedure (for all selected DMA specimens in both tests, fatigue and relaxation modulus) should be completed in a period of less than three weeks. After this period, all the specimens that have not been used should be stored in a cold room at 10ºC in order to retard aging. If these specimens are going to be used, they should be removed from the cold room at least one night before the day of testing.

8 TEST PROCEDURE

Note: The relaxation test is a nondestructive procedure. If relaxation test parameters are required, it is possible to perform this test on a specimen before performing an oscillation test. This means that after finishing the relaxation test, the same installed sample can be used for oscillation. This suggestion applies to both dry and moisture-conditioned specimens. For details on the relaxation test procedure, refer to the relaxation modulus test section (Section 8.2).

8.1 Shear oscillation (fatigue)

8.1.1 Verify if the air supply is on (30 psi).

8.1.2 Remove the bearing lock if applicable.

8.1.3 Turn on power to the electronics control box.

8.1.4 Open the instrument control software on the computer.

8.1.5 Install the correct geometry on the DMA.

8.1.6 If applicable, calibrate the instrument (bearing friction, clamp, and inertia).

8.1.7 Zero the gap.

8.1.8 Insert the DMA specimen into the holders (see Figure B.3).

FIGURE B.3—Installation of the Specimen in the DMA

8.1.9 Tighten the screws/bolts to secure the sample (do not over tighten, or stripping of the screws/bolts will occur).

8.1.10 If running a test at a temperature other than room temperature, close the temperature chamber around the sample. Be sure the sample fits into the chamber without touching the walls.

8.1.11 Zero the normal force. Be sure to zero the actual force on the sample, not the force transducer.

8.1.12 In the computer software:

- Select the DMA test geometry. Input the required data (height and diameter of DMA specimen, sample ID, etc.) (only if required by the software). Go to oscillation (if running a fatigue test). And define the two required oscillation procedures (low and high strain/stress procedures) as follows.

Low-strain/stress recommended values:

- Frequency: 10 Hz.
- Strain (or stress) amplitude: According to the homogeneity concept, the ratio of stress response to any applied strain should be independent of the strain magnitude for the linear viscoelastic region. This strain amplitude can be found performing the strain sweep test and monitoring the dynamic modulus as the strain increases. A typical value is 0.001 percent for controlled-strain tests and 3.20×10^{3} Pa for controlled-stress tests.
- Duration: 2 min.
- Sampling rate: sample every five cycles, taking at least 128 points per cycle or as many as possible if less than 128.
- Temperature (if applicable): ensure that the sample has reached equilibrium with the set temperature.

High-strain/stress recommended values:

- Frequency: 10 Hz.
- Strain (or stress) amplitude: selected according to strain (or stress) sweep results, based on the stiffness of the sample and maximum torque of the machine (see Annex A1). Typical values are 0.1–0.2 percent for controlled-strain tests and 9.08×104–1.65×105 Pa for controlled-stress tests. The high strain/stress selected should allow achieving a fatigue life longer than 30 min but less than 5 h.
- Duration: until evident failure of the sample occurs, but it must meet the above criteria.
- Sampling rate: sample every five cycles, taking at least 128 points per cycle or as many as possible if less than 128.
- Temperature (if applicable): ensure that the sample has reached equilibrium with the set temperature.
- Start the test with the applicable oscillation test procedure.
- Verify if sine waves are smooth after a few oscillations; otherwise, cancel the test immediately and start over. Rough sine waves indicate that the machine is not able to reach the desired strain at the desired frequency. If necessary modify inputs.
- Stop the test after failure occurs. Failure can be identified as a sharp drop in the dynamic modulus and phase angle. Wait until the dynamic modulus stabilizes at the lower value before stopping the test. If failure does not occur before the maximum suggested time of 8 h, it is the operator's decision to continue the test until failure or terminate the test.

8.1.13 Loosen screws/bolts and raise the machine head to remove the specimen (if running a test at other than room temperature, the temperature chamber will need to be opened first).

8.2 Relaxation modulus test

Repeat steps 8.1.1–8.1.11 of the shear oscillation procedure test.

In the computer software:

- Select the DMA test geometry.
- Input the required data (height and diameter of the DMA specimen, sample ID, etc.) (only if required by the software).
- Go to oscillation (if running a fatigue test).
- Select the option for the relaxation test procedure.
- Enter the following recommended minimum parameters:

Frequency: 10 Hz.

Strain amplitude: According to the homogeneity concept, the ratio of stress response to any applied strain should be independent of the strain magnitude for the linear viscoelastic region. This strain amplitude can be found by performing the strain sweep test and monitoring the dynamic modulus as the strain increases. A typical value is 0.001 percent.

Duration: 2 min.

Sampling rate: sample every five cycles, taking at least 128 points per cycle or as many as possible if less than 128.

Temperature (if applicable): be sure the sample has reached equilibrium with the set temperature.

Review if the particular machine that is being used requires more parameters and introduce them.

8.3 Test termination

8.3.1 Loosen screws/bolts and raise the machine head to remove the specimen (if running a test at other than room temperature, the temperature chamber will need to be opened first).

8.3.2 If a fatigue test is going to be performed on the same specimen, follow step 9.12 for the oscillation test described in the first part of this section.

9 DATA ANALYSIS

9.1 Relaxation modulus test

9.1.1 Plot relaxation modulus (E) versus time (t).

9.1.2 Fit the curve obtained in 9.1.1 using the power law relationship ($E(t) = E_\infty + E_1 t^{-n}$) (see Figure B.4).

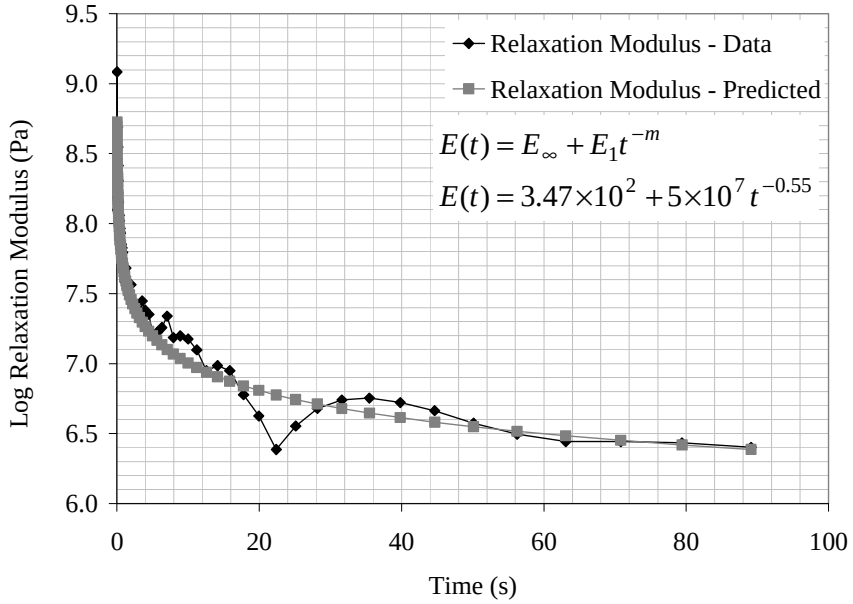

FIGURE B.4—Relaxation Modulus versus Time

9.2 Oscillation test

9.2.1 Pick the linear viscoelastic (LVE) material properties (dynamic modulus and phase angle) from the low-amplitude test. Use average values.

9.2.2 Select specific cycles from the high-amplitude test related to fatigue life (the maximum point from the relationship between G^*/G_0 versus the number of load cycles, where G^* is the dynamic modulus and G_0 is the initial dynamic modulus), as in Figure B.5. The selected cycles should be the initial cycle, and the cycles, related to 5, 10, 20, 30, 40, 50, 60, 70, 80, 90, 100, and 110 percent of fatigue life (a total of 13 cycles).

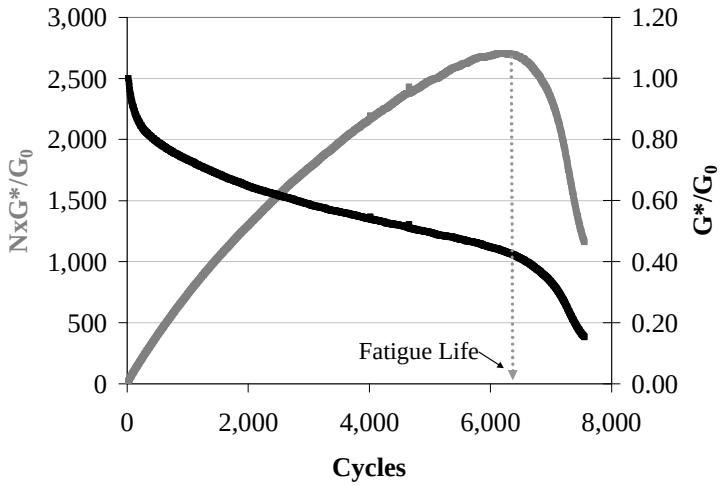

FIGURE B.5—Determination of Fatigue Life

9.2.3 Calculate, for each of the 13 selected cycles from the high-amplitude test, pseudo-strain values according to Equations 2 and 3:

Controlled strain
$$\gamma^R = \frac{G^*_{VE}\gamma_{0F}\sin(wt+\delta_{VE})}{G_R} \quad (2)$$

Controlled stress
$$\gamma^R = \frac{G^*_{VE}\gamma_{0NF}\sin(wt-\delta_{NF}+\delta_{VE})}{G_R} \quad (3)$$

where

γ = strain,
w = circular frequency ($2\pi f$),
t = time,
δ = phase angle,
G_R = reference modulus,
F = labeled quantities associated with the fatigue test,
N = parameter that is changing during each loading cycle, and
VE = material viscoelastic properties that the material would attain if it did not exhibit damage at the strain and stress levels used in the fatigue test.

G_R is determined by:

$$G_R = \frac{(\max Stress - \min Stress)}{(\max Strain - \min Strain)} \quad (4)$$

G_R is calculated for the cycle relative to 5 percent (keep the same value for the calculations of the following percentages). For each cycle, locating approximately 128 data points inside the cycle is recommended. For simplicity, G_{VE} is considered equal to G_R.

9.2.4 Plot the relationship between pseudo-strain and stress for each cycle chosen from the high-amplitude test (see Figure B.6). The approximately 128 points collected in each cycle will allow the construction of the areas in Figure B.6.

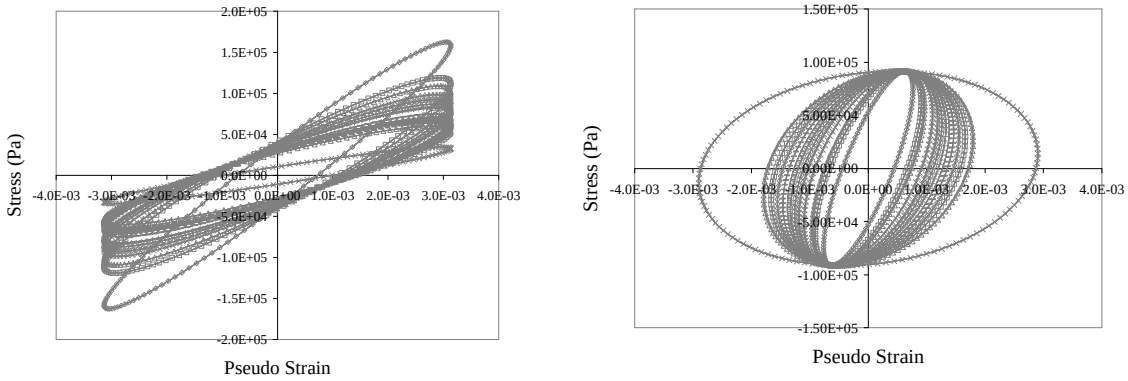

(a) (b)

FIGURE B.6—Hysteresis Loop for Controlled Strain (a) and Controlled Stress (b).

9.2.5 Calculate the area of the plots generated in step 9.2.4. This area is the actual hysteresis loop area, which represents the dissipated pseudo-strain energy (DPSE) for each cycle.

9.2.6 Calculate WR1 using Equations 5 and 6. This DPSE component accounts for the damage that causes an increase in the apparent phase angle and an increase in the hysteresis loop area with respect to a reference modulus that represents the intact undamaged material.

Controlled strain $$W_{R1} = \pi G^*_{VE} \gamma^2_{0F} \sin(\delta_{NF} - \delta_{VE}) \quad (5)$$

Controlled stress $$W_{R1} = \pi \frac{\tau^2_{0F}}{G^*_{VE}} \sin(\delta_{NF} - \delta_{VE}) \quad (6)$$

where

τ = used stress amplitude.

9.2.7 Calculate WR2 using Equations 7 and 8. This DPSE component accounts for the nonuniform energy dissipation within the hysteresis loop (difference between the actual and the idealized hysteresis loop area). Do not consider this step if data points within each cycle is not available.

Controlled strain $$\left(\text{Area of Stress - Pseudo StrainLoop} / \frac{G^*_N}{G^*_{VE}} \right) - W_{R1} \quad (7)$$

Controlled stress $$\left(\text{Area of Stress-Pseudo Strain Loop} \times \frac{G^*_N}{G^*_{VE}} \right) - W_{R1} \quad (8)$$

9.2.8 Calculate WR3 using Equations 9 and 10. This DPSE component is associated with the difference between the pseudo-stiffness of the undamaged material and the pseudo-stiffness after damage.

Controlled strain $$W_{R3} = \frac{1}{2}\gamma_{0F}^2 (G^*_{VE} - G^*_{NF}) \quad (9)$$

Controlled stress $$W_{R3} = \frac{1}{2}\tau_{0F}^2 \left(\frac{1}{G^*_{NF}} - \frac{1}{G^*_{VE}} \right) \quad (10)$$

9.2.9 Sum WR1, WR2, and WR3 calculated from steps 9.2.6, 9.2.7, and 9.2.8. If step 9.2.7 was not considered, calculate just the sum of WR1 and WR3.

9.2.10 Plot WR1+WR2+WR3 versus the log of the number of load cycles (N) (Figure B.7). If you did not consider step 9.2.7, plot only WR1+WR3.

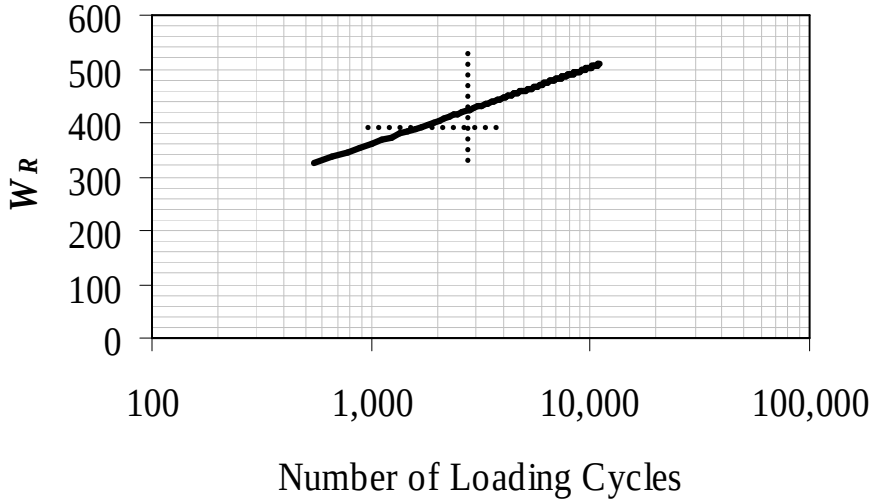

FIGURE B.7—W_R versus Number of Load Cycles

9.2.11 Select the b value from the plot in step 9.2.10. The b value is the slope of the plot.

9.2.12 Calculate R(Nf) values using Equation 11.

$$R(Nf) = \left[(2n+1)^{n+1} \left(\frac{G_R b}{4\pi E_1 \Delta G f} \right)^n N \right]^{\frac{1}{2n+1}} \quad (11)$$

where

n = $1/m$ for controlled-strain tests and $1+1/m$ for controlled-stress tests,
m = exponent of time in the power law equation of the relaxation modulus,
E_1 = relaxation modulus-time relationship,
ΔGf = bond energy,
N = number of cycles to failure, and
G_R = reference modulus.

10 KEYWORDS

Dynamic mechanical analyzer (DMA), fatigue test, relaxation modulus, damage, dissipated energy.

ANNEXES

A1. STRAIN/STRESS SWEEP TEST FOR DETERMINING THE HIGH STRAIN AMPLITUDE FOR THE OSCILLATION TEST

A1.1. In the computer software:

A1.1.1. Go to oscillation.
A1.1.2. Select the amplitude sweep test.
A1.1.3. Strain/stress sweep test recommended values:

- Strain/stress range: the strain range is 0.001–0.6 percent, and the stress range is 1.1×10^3–2.0×10^5 Pa. The amplitude range should go from very low values (on the linear region) to values high enough to check nonlinear and damage behaviors.
- Delay time: 2 s.
- Number of samples: 25.
- Number of periods: 200.
- Number of points per period: 8,192.
- Temperature and frequency: selected by the operator.

A1.2. Data analysis

A1.2.1. Monitor the strain/stress amplitude responses (slopes of strain/stress versus time plots). These slopes are determined by plotting the strain/stress amplitude for each of the 200 load applications and fitting a linear trend line. For strain sweep tests, positive slopes represent strain hardening, slopes close to zero represent nonlinear viscoelastic behavior, and negative slopes represent damage. For stress sweep tests, negative

slopes represent strain hardening, slopes close to zero represent nonlinear viscoelastic behavior, and positive slopes represent damage.

A1.2.2. Select the strain/stress amplitude that corresponds to the limit for the dynamic modulus and the phase angle that marks the end of the nonlinear viscoelastic region and the start of the damage region. This amplitude is selected fitting the data with a horizontal line ($y = \alpha_0$) connected at the point x_0 to a linear ($y = b_0 + b_1 x$) for the strain sweep case (see Figure B.8) or the quadratic function ($y = \beta_0 + \beta_1 x + \beta_2 x^2$) for stress sweep case (see Figure B.9). This specific strain/stress amplitude should be used for the shear oscillation test (fatigue).

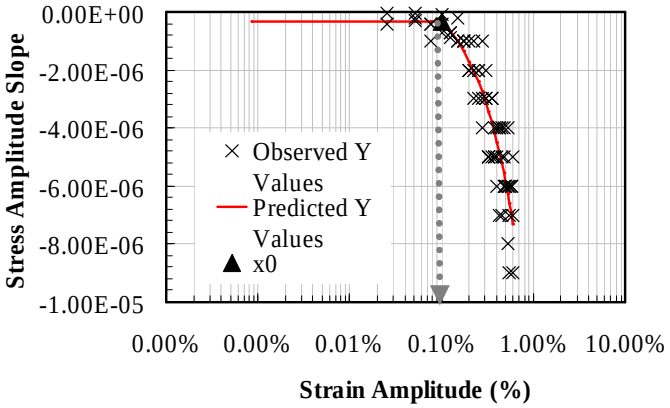

FIGURE B.8—Stress Amplitude Slope versus Strain Amplitude, Strain Sweep Test

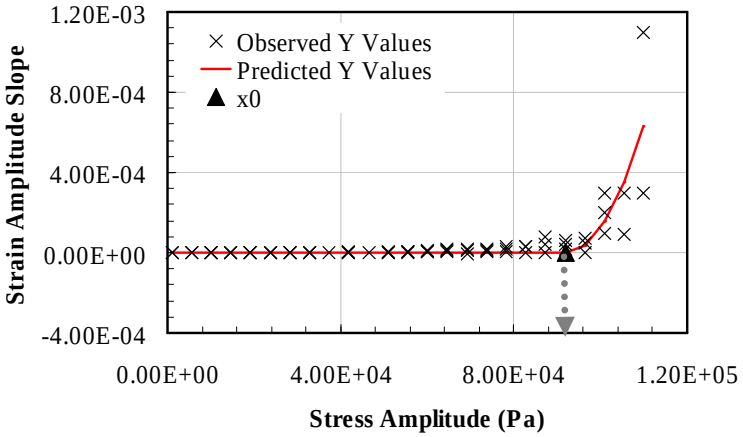

FIGURE B.9—Strain Amplitude Slope versus Stress Amplitude, Stress Sweep Test

VITA

Name: Pedro Cavalcanti de Sousa

Address: Department of Civil Engineering
Texas Transportation Institute
CE/TTI Building, Room 501H
3135 TAMU
College Station, TX 77843

Email Address: pedro.sousa203@gmail.com

Education: B.E., Universidade Fedral do Ceará, Brazil, 2008

M.E., École Centrale de Lyon, France, 2008

M.S., Texas A&M University, 2010